

**NUMERICAL SIMULATION OF WEATHER OVER KENYA USING THE
WEATHER RESEARCH AND FORECASTING –ENVIRONMENTAL
MODELLING SYSTEM**

BY

PHILIP OBAIGWA SAGERO

156/78590/2009

**A Dissertation submitted in partial fulfillment of the requirements for the Degree of
Master of Science in Meteorology**

**DEPARTMENT OF METEOROLOGY
SCHOOL OF PHYSICAL SCIENCES
UNIVERSITY OF NAIROBI**

2012

DECLARATION

I hereby declare that this dissertation is my original work and has never been presented for a degree in any other University

Signature

Date


.....

15/06/2012
.....

PHILIP OBAIGWA SAGERO
Department of Meteorology
University of Nairobi
P.O Box 30197
Nairobi, Kenya.

This Dissertation has been submitted for Examination with our approval as university supervisors;

Signature

Date

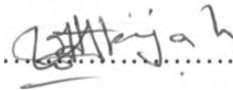

.....

18/06/2012
.....

Dr. JOSEPH M. ININDA
Department of Meteorology
University of Nairobi
P.O Box 30197
Nairobi, Kenya.

Signature

Date


.....

18/6/12
.....

Dr. FRANKLIN J. OPIJAH
Department of Meteorology
University of Nairobi
P.O Box 30197
Nairobi, Kenya.

ABSTRACT

This study investigated the accuracy and skill of the Weather Research and Forecasting-Environmental Modelling System (WRF-EMS) to simulate weather over Kenya. The study period was March to May 2011, a long rain season. The data used in the study included the observed daily rainfall and temperature for 27 stations over Kenya, obtained from Kenya Meteorological Department and initialization data for WRF-EMS obtained from the Global Forecasting Model (GFS). Model simulation was done for the period of study and the model output for the 27 stations was used to determine the performance of the WRF-EMS model over Kenya in terms of skill and accuracy.

The methods of analysis included spatial distribution comparison, correlation analysis, absolute mean error, root mean square error analysis and categorical statistics.

Analysis of the simulated and observed spatial distribution of rainfall over the study area indicated that the WRF model was capable of reproducing the observed general pattern, although in some cases the model displaced the location of occurrence of maximum rainfall. The spatial pattern of the observed temperature was well captured by the WRF model.

Correlation between the forecasted and observed rainfall indicated significant values over most stations when the entire season was considered. On monthly basis the high correlation were observed in March while they were relatively low in April and May. This was attributed to more localized systems that is associated with Rainfall for April and May which may not have been captured by the model. Similar correlation results were noted for temperature.

Root Mean Square Error (RMSE) and Absolute Mean Error (AME) values were generally small for most of the stations for both the rainfall and temperature, which is an indication of small deviation of the forecasted values compared to observed. Categorical statistics that included Frequency Bias Index (FBI), Equitable Threat Score (ETS) and True Skill Statistic (TSS) indicated higher skill of the model for the low threshold of less than 1mm/day of rainfall, implying that the model was able to detect the occurrence of rainfall but failed to determine the

exact amounts. This was also in line with the fact that the hit rate for most of the stations was higher than 50% for low threshold of less than 1mm/day.

Overall, the model has skill in forecasting both rainfall and temperature but may fail to give the exact location of occurrence of storms, therefore, during the months of enhanced rainfall in the months of April and May the model forecast needs to be complemented by other models or forecast methods. There is therefore, need to improve its performance over the domain through reviewing the parameterization of small scale physical processes and its ability in simulating weather on the medium and long range scale.

TABLE OF CONTENTS

DECLARATION	ii
ABSTRACT.....	iii
TABLE OF CONTENTS	v
LIST OF FIGURES AND THEIR CAPTIONS.....	vii
LIST OF TABLES	ix
CHAPTER ONE	1
INTRODUCTION	1
1.0 Background	1
1.1 Problem Statement	2
1.2 Objectives.....	3
1.3 Justification	3
1.4 Region of Study.....	4
1.4.1 Physical Features of the Study Area.....	4
1.4.2 Climatology of the Area of study	5
CHAPTER TWO	8
LITERATURE REVIEW.....	8
CHAPTER THREE.....	15
MODEL APPLIED, DATA AND METHODOLOGY.....	15
3.0 INTRODUCTION.....	15
3.1 Weather Research and Forecasting - Environmental Modeling System	15

3.3 Data	20
3.3.1 Rainfall and Temperature data	20
3.4 METHODOLOGY.....	21
3.4.1 Data Quality Control	22
3.4.2 Assessment of the Spatial Distribution of Observed and Simulated Data.....	22
3.4.3.1 Correlation Analysis.....	22
3.4.3.2 Root Mean Square Error and Absolute Mean Error (AME)	23
3.4.3.3 Verification scores.....	23
CHAPTER FOUR.....	26
RESULTS AND DISCUSSIONS.....	26
4.0 INTRODUCTION.....	26
4.1 The Performance of the Rainfall during March-May 2011 Season.....	26
4.2 Spatial Distribution of Observed and Forecasted Rainfall and Temperature.....	30
4.3. Results from Assessment of Model Accuracy and Skill	41
4.3.1 Results From the Analysis of the Model Accuracy	42
4.3.2 Measure of the Skill	46
CHAPTER FIVE	51
SUMMARY, CONCLUSIONS AND RECOMMENDATIONS	51
5.0 Summary	51
5.1. Conclusion.....	52
5.2 Recommendations	52
6.0 ACKNOWLEDGEMENTS	54
7.0 REFERENCES.....	55

LIST OF FIGURES AND THEIR CAPTIONS

FIGURE	TITLE	PAGE
Figure 1:	A map of Kenya (sourced from Macmillan Kenyan Secondary School)))Atlas,1999) .	5
Figure 2:	Main Components of WRF-EMS Model	16
Figure 3:	Systems of WRF-EMS Model.....	17
Figure 4:	WRF vertical coordinate	19
Figure 5:	Study area showing the location of stations used in the analysis.....	21
Figure 6:	The rainfall performance of March-May 2011 season.....	27
Figure 7:	The rainfall performance of March-May 2011 season.....	27
Figure 8:	the general circulation for March, 2011 at 700mb level.....	29
Figure 9:	the general circulation for May, 2011 at 700mb level.....	30
Figure 10:	The observed and forecasted rainfall for the March-May 2011 season	31
Figure 11:	The Observed and Forecasted rainfall for the month of March 2011	31
Figure 12:	The Observed and Forecasted rainfall for the month of April 2011	32
Figure 13:	Observed and Forecasted rainfall for the month of May 2011.....	32
Figure 14:	The observed and forecasted temperature for March-May 2011 season.....	33
Figure 15:	The observed and forecasted temperature for the month of March 2011	33
Figure 16:	The observed and forecasted temperature for the month of April 2011	34
Figure 17:	The observed and forecasted temperature for the month of May 2011.....	34
Figure 18:	spatial distribution of Rainfall for the March-May 2011 season (a) Observed Rainfall (b) Forecasted Rainfall.....	35
Figure 19:	Spatial distribution of Rainfall for the month of March 2011 season (a) Observed Rainfall (b) Forecasted Rainfall.....	36
Figure 20:	Spatial distribution of Rainfall for the month of April 2011 season (a) observed Rainfall (b) Forecasted Rainfall.....	36

Figure 21: Spatial distribution of Rainfall for the month of May 2011 season (a) observed Rainfall (b) Forecasted Rainfall.....	37
Figure 22: Spatial Distribution of Rainfall for March 6th 2011 (a) Observed (b) Forecasted	37
Figure 23: Spatial Distribution of Rainfall for May 1 st 2011 (a) Observed rainfall (b) Forecasted rainfall.....	38
Figure 24: Spatial Distribution of temperature for March 2011 (a) Observed temperature (b) Forecasted Temperature.....	39
Figure 25: Spatial distribution of temperature for April 2011 (a) Observed temperature (b) Forecasted temperature	39
Figure 26: Spatial distribution of temperature for May 2011 (a) Observed temperature (b) Forecasted temperature	40
Figure 27: time series for MAM, 2011 season for Malindi station.....	41
Figure 28: time series for MAM, 2011 season for Kitale station.....	41
Figure 29: Percentage correct for the forecast for March-May 2011 rainfall season	50
Figure 30: Percentage correct of the forecast rainfall for the month of March-May 2011	50

DEPT. OF METEOROLOGY UNIVERSITY
OF NAIROBI

LIST OF TABLES

Table 1: WRF-EMS model physics and dynamics configurations.....	20
Table 2: A 2 by 2 Contingency Table.....	24
Table 3: Correlation Coefficient (CC), Absolute Mean Error (AME) and Root Mean Square Error (RMSE) for Rainfall for March, April and May	43
Table 4: Correlation Coefficient (CC), Absolute Mean Error (AME) and Root Mean Square Error (RMSE) for Temperature for March, April and May.....	45
Table 5: Frequency Bias Index (FBI) for Rainfall.....	47
Table 6: Equitable Threat Score for Rainfall.....	48
Table 7: True skill statistics for Rainfall.....	49

LIST OF ACRONYMS USED IN THE TEXT

AME	Absolute Mean Error
AMSL	Above Mean Sea Level
ARW	Advance Research WRF
CC	Correlation Coefficient
EALLJ	East Africa Low Level Jet
EMS	Environmental Modelling System
ETS	Equitable Threat Score
FBI	Frequency Bias Index
GFS	Global Forecasting Model
GTS	Global Telecommunication System
ITCZ	Inter-Tropical Convergence Zone
LAM	Limited Area Model
LTM	Long Term Mean
MAM	March April May season
NCAR	National Center Of Atmospheric Research
NCEP	National Centers for Environmental Prediction
NMM	Non-Hydrostatic Mesoscale Model
NWP	Numerical Weather Prediction
RAMS	Regional Atmospheric Modelling System
RMSE	Root Mean Square Error
TSS	True Skill Statistic
WRF	Weather Research and Forecasting
WSF	WRF Software Framework

CHAPTER ONE

INTRODUCTION

1.0 Background

Previous methods of forecasting the weather patterns over Kenya were mainly based on synoptic chart analysis. Under this method, all the weather observations from different stations are plotted on special charts and analyzed. However, the chart analysis is a subjective method and occasionally does not give accurate predictions of weather especially when the weather activities are associated with meso-scale systems. Low skill of weather forecasting renders it limited utility.

Recent advancement in numerical methods has led to the adoption of dynamical models, which incorporate the physics of atmospheric processes. The advancement in Numerical Weather Prediction (NWP) has been possible through the utilization of fast data processing that simulates the physics of the atmosphere from complex mathematical equations. High-speed computers have made it feasible for numerical models to perform complex parameterization of physical processes and include increased horizontal resolution that generate high temporal and spatial details of the evolution of events at the synoptic and sub-synoptic scale (Brooks and Doswell, 1999). Internet has also made it possible to run the model online. With the advancement in communication system and availability of regional models, many of National Meteorological Service Centers have access to NWP models.

WRF-EMS is a numerical weather prediction (NWP) model with sufficiently high horizontal and vertical resolution to forecast meso-scale weather phenomena. Meso-scale systems are often forced by topography or coastlines, or are related to convection. These systems present some of the most difficult forecasting challenges because of their small space and time scales. On the other hand severe weather occurs at the meso-scale, including tornadoes and meso-scale convective systems. Visibility, turbulence, sensible heat, and sea state can vary enormously over just a few kilometers and have a tremendous impact on operations. In weather analysis one will

frequently depend on guidance from mesoscale models, particularly in tactical situations where real-time weather observations are sparse or nonexistent.

Despite these high-speed computers, inaccurate weather forecasts still exist due to errors from the chaotic nature of the atmosphere, the inexact equations of motions, and gaps in specifying the initial state of the atmosphere. Accurate weather prediction is not only useful in disaster mitigation but also in increasing production of food, water resource management, hydropower production among others. Although weather forecasting is essential for any country, it is limited by inaccuracies in forecasting methods. There have been efforts in recent days to improve the accuracy of the forecasts, through the use of mesoscale model with high horizontal and vertical resolutions. This is because rainfall can only be predicted with accuracy using fine grid models.

Another major hurdle for mesoscale modeling is the verification of the direct model output against the observed. Observed data for small-scale weather phenomena are either not available, unevenly distributed, or provide incomplete coverage

The information contained in the observations may not give the same information as the model without some preconditioning (Cherubini *et al.*, 2002). Mesoscale NWP models are by their formulation still deterministic. Their predictability horizon generally does not exceed their short lifetime. This implies that direct model output at the smallest scales should always be interpreted probabilistically. If the information at these scales is essentially probabilistic then, a deterministic interpretation and verification is inappropriate.

1.1 Problem Statement

Kenya is prone to extreme weather/climate events such as droughts and floods that are often associated with severe and adverse social and economic impacts. These impacts include famine, water scarcity, rationing of electricity, conflict over pasture, human wildlife conflicts, floods and shortage of many other basic needs. Such impacts retard the economic growth and development of a country. Therefore accurate prediction of weather/climate at the short and long range and timely early warning are among the strategies necessary for preparedness and mitigation of weather and climate related disasters in the country.

The main purpose of weather forecasting is to provide timely information on the actual and expected weather and advice on its likely impact on the various day to day operations in various sectors. Occurrence of severe weather has adverse effect to the community. Sometime severe weather mostly is localized, and therefore, the forecast should be skillful. However, the utility of the forecast depend on the skill of the model.

Rainfall has always been of interest to forecasters because it influences daily life. Recent floods and mudslides over Kenya emphasize how important it is to know how models can reproduce these events. Skillful prediction of severe weather is important for optimal planning and management of all weather-related activities. The usefulness of the weather forecast increases with resolution, the model that are able to predict the occurrence of severe thunderstorm are more desirable

The main question to answer was how well the WRF-EMS model accurately predicts severe weather.

1.2 Objectives

The main objective of this study was to simulate the rainfall and temperature distribution over Kenya using the WRF-EMS model.

To achieve this main objective, the following specific objectives were pursued.

1. Analyze the performance of the rainfall during the March-May season for the year 2011
2. Simulate the precipitation and temperature over Kenya using the Weather Research and forecasting (WRF EMS) Model
3. Determine the accuracy and skill of the WRF EMS model.

1.3 Justification

Rainfall is one of the main weather elements that are very important to the economy of any country. Understanding the performance of rainfall for a given season, helps in understand the circulation of the local and synoptic scale systems that may have caused the performance.

Forecasting severe thunderstorms is one of the most difficult tasks in weather prediction, due to their rather small spatial and temporal extension and the inherent non-linearity of their dynamics and physics (Orlanski, 1975). Numerical modelling has made substantial advances in the modelling of convective clouds and mesoscale convective systems (Hobbs, 1991). To know the capability of the model it is important for simulation to be done, so as critical analysis of the model can be looked at.

An accurate, location specific and timely prediction is required to avoid loss of lives and property due to strong winds and heavy precipitation associated with such weather systems

1.4 Region of Study

The area of focus for this study is Kenya, as shown in Figure 1. The area lies approximately between longitudes 34°E-42°E, and latitudes 5°N-5°S with a total area of about 582650 km². It is a country in East Africa bordering Somalia to the east, Ethiopia to the north, Tanzania to the south, Uganda and Lake Victoria to the west, southern Sudan to the North West, and The Indian Ocean to the south east. The Equator passes through the country in an east-west direction.

1.4.1 Physical Features of the Study Area

The region has complex topographical features, which include the highlands and Great Rift Valley. The relief map of Kenya indicates that quite a large portion of the area lies around 1200 m above mean sea level (AMSL). The highest mountains in Africa are found in this region. These mountains include Kenya (5199 m), Kilimanjaro (5895 m), Elgon (4321 m), Aberdare ranges (3999 m), and Mau Escarpment (3098 m).

Considerable spatial variations of climate occur throughout the region due to the great diversity of topography and the presence of large water bodies like the Indian Ocean and Lake Victoria (Indeje, 1994; Song *et al.*, 2003). The complex mountains are also the source of watersheds for some of the major rivers of the region (Krishnamurti and Ogallo; 1989). The mountains, therefore, form an integral component of the regional hydrological cycle. Lake Victoria, Turkana, and the Great Rift Valley are some of the features in the area. Certainly, these local factors significantly influence the local circulation pattern and hence the local climate.



Figure 1: A map of Kenya (sourced from Macmillan Kenya Secondary School)

1.4.2 Climatology of the Area of study

Climate conditions in Kenya vary considerably from place to place due to differences in topography and the presence of water bodies such as the Indian Ocean and Lake Victoria. Precipitation is the parameter that has the highest space-time variability. On average more than

800 mm of annual rainfall is observed over areas bordering Lake Victoria to the west, and the Indian Ocean to the east. The highlands of central Kenya also receive rainfall of more than 800 mm per year, with the northern and eastern parts of Kenya, which is semi-arid, receive less rainfall.

The climate of this region varies from arid, humid, equatorial type near the Equator to the tundra climate found over high and snow-capped mountains. The humid climates are concentrated over the highlands, around the Lake Victoria and along some of the coastal areas. The remaining areas are, however, arid or semi-arid. These dry areas are in the latitudes dominantly under the influence of low-level subsiding and diffluent monsoonal flow (trade wind inversion).

The rainfall season in Kenya is divided into two seasons (Vyazilova 2001). These include the primary rainy season (March-May) known as the "long-rains" season and the secondary rainy season (September-December) locally called the "short-rains" season. These rainy seasons coincide with periods of the year when the ITCZ is passing over this part of the continent. The intervening periods are relatively dry. However, there are rainfall-enhancing mechanisms in the region which contribute to substantial rains over the western and coastal parts of East Africa in July/August. These mechanisms include the warm and moist Congo air mass, and the East Africa low level jet (EALLJ) respectively.

The East African Low Level Jet is the most important among the jet streams as a rainfall mechanism over the region. The EALLJ is located at 1-1.5km above mean sea level, with core speed of 13 meters per second, width 200-400km, length 500-100km, and depth of about 1km (Findlater, 1969). It is estimated to transport 7×10^{10} kg/s of atmospheric mass across the equator, and therefore is an effective transporter of water vapor (Rao *et al.*, 1981). It is strongest in northern hemisphere summer when it penetrates the coastal regions of East Africa, resulting in heavy rainfall over the coastal areas during July to August period.

The Monsoon circulation also account for the rainfall that is received in the region. Kenya experience two monsoon wind systems , namely northeast and southeast monsoon (Findlater, 1971). Many extreme rainfall anomalies in the region during the major rainy season have been associated with anomalies in the monsoon wind systems, since they are major transport

mechanism of moisture into the region (Findlater, 1969). The characteristics of these winds over the region are controlled by the location, intensity and orientation of major semi-permanent anticyclones of Africa, together with other related general circulation parameters (Kiangi *et al.*, 1981).

Tropical cyclones also control the weather of a region by shifting the ITCZ from its normal position towards the location of the cyclones, resulting into dry weather over the expected wet areas and above normal rainfall over areas favored by the cyclone activities (Anyamba and Ogallo, 1985). The presence of tropical cyclone in the Mozambique channel during late March or in early April, delay the onset of long rains season in East Africa.

The varied Topography of the region of study, proximity of the Indian Ocean and the location of the vast Lake Victoria in the central part of East Africa give rise to meso-scale circulation which have significant contributions towards the complex weather patterns observed over Kenya. A study by Mukabana (1992) have demonstrated that the spatial distribution of weather and climate over Kenya is to a large extent determined by the interaction between the quasi-stationary mesoscale circulations systems and the seasonally varying large scale flow.

CHAPTER TWO

LITERATURE REVIEW

Asnani and Kinuthia (1979) found from an observational analysis that the diurnal variation of the rainfall in Kenya is largely determined by the mesoscale flow, synoptic scale flow, convective instability and interaction between the mesoscale and synoptic scale flow. Okeyo (1987) showed that mesoscale convergence concentrates moisture in localized regions. He found that the most important factors influencing hailstorm activity over the highlands are the Lake Breeze and upslope/down slope circulations. He also found that cumulus convection enhances the mesoscale circulations over the region.

Mukabana (1992) reported that non-linear scale interactions between large-scale monsoon currents and the local circulation are vital components to the development of weather patterns in Kenya. Indeje (1993) and Mutai (1998) showed that modification of the land surface characteristics such as surface roughness and albedo through human activities like deforestation and overgrazing would have considerable impacts on the meso-scale weather systems in the region.

Pielke (1974) examined the effect of surface roughness on meso-scale (land/sea breeze) flow over South Florida and concluded that the differential roughness between land and water does not by itself play an important role in the magnitude of convergence. Indirectly, however, the surface roughness has an influence on the magnitudes of convergence through increased turbulent transfer of heat.

Okeyo (1982) used a two-dimensional, hydrostatic, primitive equation model, which was one of the predecessors to RAM (Regional Atmospheric Modeling System) to study the meso-scale circulation over Kenya. He reported that the meso-scale flows in the form of the lake Victoria breeze, the upslope wind and the Indian Ocean breeze converge above the Nandi-Kericho highland area where hailstorm are observed almost daily. He further showed that the combined lake/land and sea/land breezes and upslope and down slope winds produce a more intense circulation during both day and night than the lake/land and sea/land breezes over a flat terrain

Opijah (2000) carried out numerical simulation of the impact of urbanization on the microclimate over Nairobi area. He found that the major influence on the weather/microclimate in cosmopolitan Nairobi province is topography. Although comparatively smaller than the forcing through topography, the impact of the land use/ land cover changes like the urban built up area and forest are substantial in spite of the relatively small areas currently occupied by forests.

Epstein (1969) developed a stochastic dynamic prediction scheme that included a forecast equation for probability distribution of the atmosphere variables. Because of the size of the problem this method is unfeasible except for the simplest models

Indeje *et al.*, (2001) employed the National Center for Atmospheric Research Regional Climate Model (RegCM) to study the dynamics of the Turkana low-level jet that lies between the Ethiopian Highlands and the East African Highlands, and also investigate the mechanisms responsible for the observed dry condition over Lake Turkana basin that lies in the wider section of the Turkana channel. They found that orographic forcing is the most important factor in the formation and maintenance of the jet. Besides, the large-scale monsoon background flow is important in determining the wind speed in the jet cores, and the depth of the channel determines the vertical structure and location of the jet core.

Ghell and Lalaurette (2000) analyzed model performance using a high-resolution-observing network over France. They found that gridded observation better represent the grid box behavior described by the Model. Skilly and Handerson (1996) pointed out that when dealing with variables that are implicitly areal (as they result from sub-grid parameterizations like convection, precipitation, radiation among others), a single number is usually inadequate for evaluating all the desired information about the performance of an analysis-forecast system.

Mohantya and Litta, (2010) carried out a numerical simulation of a tornado over Ludhiana in India using WRF-NMM model. They found that the model simulated well the meteorological parameters including; relative humidity, mean sea level pressure, rainfall, moisture convergence, pressure vertical velocity and surface wind speed that are favourable for tornado formation and agreed reasonably well with the observations. This shows the capability of high resolution model in forecasting severe thunderstorms, which is highly localized

Previous model validation studies have used conventional statistics to measure the similarity between observed and modeled data. Taylor *et al.*, (2001); and Boer and Lambert (2001) characterized model performance from correlation, root mean square (RMS) error, and variance ratio. Both studies found similar ways to combine these three statistics in a single diagram, resulting in nice graphical visualizations of model performance. This approach, however, is only practical for a small number of models and/or climate quantities. In addition, Taylor's widely used approach requires centered RMS errors with the mean bias removed. However, the mean bias is considered an important component of model error. Murphy *et al.*, (2004) introduced a "Climate Prediction Index" (CPI), which measures the reliability of a model based on the composite mean square errors of a broad range of climate variables. More recently, Min and Hense (2006) introduced a Bayesian approach into model evaluation, where skill is measured in terms of a likelihood ratio of a model

Lilly, 1990 did a study on NWP and found that at high resolution, convection is explicitly resolved, meaning that clouds and precipitation are entirely represented through additional prognostic equations which account for the microphysical and thermo dynamical transformations associated with water phase changes. Moreover, high resolution allows for a much more detailed representation of the orographic forcing, known to play a major role at the mesoscale. One major expectation from these new numerical tools is a better forecast of small scale meteorological phenomena such as thunderstorms, squall lines, or convective rain bands, and a more reliable estimate of associated precipitation (). However, little experience has been gained so far in concluding to what extent such phenomena are predictable.

Numerical statistical methods predict precipitation on spatial scale different from the observed. Therefore, verification against irregularly distributed data, as surface synoptic observations on the global telecommunication system (GTS) might be, is liable to misinterpretation (Giorgi *et al.*, 2000). Furthermore the interpolation methods that are commonly used assume that the underlying field is continuous. This assumption is probably not suitable when dealing with finite-differentials or spectral methods that produce point, rather than areal averaged values. (Kim *et al.*, 1984) and (Karl *et al.*, 1990) treated simulated precipitation as a real quantity. Alternatively

Wigler and Santer (1990) and Wilson and Lettenmainer (1992) recommended the grid point approach for the simulated quantities.

Ebert and McBride (2000); (Done *et al.*, 2004) and (Davis *et al.*, 2006) have developed object-based methodologies which assess the positioning, intensity, and structure of precipitation forecasts. Briggs and Levine (1997); Zepeda *et al.*, (2000); (Casati *et al.* 2004) and (Bousquet *et al.*, 2006) has used spatial decomposition methods to investigate how forecast error varies with scale. Marzban and Sandgathe (2006) have used a cluster analysis method that is both object-based and spatial.

Ensemble modeling is now routinely applied on essentially all time scales, ranging from the scale of weather forecasts to the scale of climate-change scenarios, and its success has been demonstrated in many studies (e.g. Palmer *et al.* 2004). Simple ensemble-models can be constructed by pooling together the available single model predictions with equal weight. However, given that models may differ in their quality and skill, it has been suggested to further optimize the effect by weighting the participating models according to their prior performance (e.g. Giorgi and Mearns 2002).

The technique of ensemble modeling is used with great success at forecasting centers around the world (Tracton and Kalnay, 1993). Richardson in 2000 showed that probability forecasts derived from an ensemble prediction system are of greater benefit than a deterministic forecast produced by the same model. In its simplest form, model ensemble forecast is produced by simply merging the individual forecasts with equal weights. Several approaches have attempted to combine model ensemble forecasts to a single reliable forecast that carries higher skills when compared to the individual member models. These include the simple ensemble mean (Peng *et al.*, 2002; Pavan and Doblas-Reyes 2000; Palmer *et al.*, 2004), regression-improved ensemble mean (Peng *et al.*, 2002; Kharin and Zwiers 2002), bias-removed ensemble mean (Kharin and Zwiers 2002), and the multimodel superensemble (Krishnamurti *et al.*, 1999). The multimodel superensemble technique showed higher skill for short range and seasonal forecasting compared with member model forecasts (Krishnamurti *et al.*, 2000a).

Webster *et al.*, 1998, discovered that the dynamical predictions suffer from a consistently large ensemble spread, which is compatible with the theory that chaotic weather systems in the Southern Hemisphere may trigger breaks in the Asian monsoon, providing short-term predictability, but limiting seasonal predictability. Zwiers *et al.*, (2000) analyzed an ensemble of 47-year simulations done with the second generation Canadian General Circulation Model (GCM2) in which the SST and sea-ice conditions were specified from observations. They found that the fraction of the atmospheric variability in mean-seasonal conditions forced by the SST variability was large in the tropics, and smaller, but still statistically significant over the northeastern Pacific and North America.

Kalnay, 2003, noted that for dynamical models, the uncertainties in model initialization can be addressed by applying ensemble techniques, i.e. by repeatedly integrating the model forward in time from slightly-perturbed initial conditions, with the perturbations being designed so that they capture as much as possible of the underlying uncertainty.

A comparative verification of the quantitative precipitation forecasts for UKMet office, NCEP and MM5 NWP models have been carried out by Gitutu (2006) over Kenya. He examined the level of skill of daily precipitation forecasts of Numerical weather prediction (NWP) models where in all the models the root mean square error was found to be largest during the rainy season of March-May and relatively low for the drier months. The root mean square error was particularly high on occasions of heavy precipitation which all the models failed to simulate for the case of Lamu and Marsabit in July. There were no other significant differences between the models that could be discerned other than slightly larger errors produced by the NCEP model.

Skill and accuracy of the quantitative precipitation forecasts by CCAM, UM and NCEP-MRF models at Mgeni catchment in KwaZulu-Natal, South Africa have been verified using various statistical scores by Beyene *et al.* 2010. In their findings, CCAM model was capable of identifying a rainfall event, but with a tendency of under-estimating its magnitude. The UM model was capable of distinguishing rainy days from non-rainy days, but with a significant over-estimation of rainfall amount. There was no significant difference between the 1 and 2 day lead time UM forecasts. Statistical comparisons showed that there was an acceptable skill in the

CCAM forecasts, but the forecast skill of the UM model was low and unreliable. Results obtained for a continuous period of 92 days showed that the NCEP-MRF rainfall forecasts were significantly over-predicted. The NCEP-MRF rainfall forecast was found to be totally unskillful, although the skill was seen to slightly increase with decreasing lead time. The combined use of the CCAM and UM models by a “weighted averaging” had little effect in improving the skill as it is overshadowed more by the over-estimation of the UM forecasts than the under-estimation of the CCAM forecasts. The ECMWF-IFS analysis shows better agreement with GPS PWV than do the NCEP–NCAR reanalyses (the RMS error is smaller by a factor of 2). The model changes in ECMWF-IFS were not clearly reflected in the PWV error over the period of study (2005–08). The results pointed to a dry bias in the ECMWF analysis in 2006 when Vaisala RS80-A soundings were assimilated, and a diurnally varying bias when Vaisala RS92 or Modem M2K2 soundings were assimilated: dry during day and wet during night. The overall bias is offset to wetter values in NCEP–NCAR reanalysis II, but the diurnal variation of the bias is observed too.

In their study to assess the predictability of short and medium range weather over the diverse regions of Africa, Mutemi *et al.* 2007 found out that bad models and poor analysis fields used during the training phase degraded the skill of the FSUSE model. Over East Africa, FSUSE model was found to capture rainfall events and resolve the physical mechanisms of rainfall as the forecasts were consistent with ITCZ. The skill scores of the FSUSE products were remarkably better than the GASP, NOGARS, GEM, JMA, GFS and ECMWF models and ensemble mean for rainfall, mean sea level pressure and u and v wind components at 200hPa and 850hPa. The superior skill of the multimodal super-ensemble and its lead time average of at least three days over that of the best member model were obtained consistently in all five different regions of the African continent considered. Lack of high quality observational and benchmark analysis fields and assuming mesoscale forcing contributed to poor skills in all the models examined

Some forecast verification work has also been done for the east African region where the skill of ECHAM4.5 over the region has been addressed by Mutemi (2003), IRI/ICPAC collaboration (2002) and Indeje (2000). The results indicated that ECHAM4.5 was the best model especially between July-December months. The skill of the model was found to be higher during ENSO when large SST values are found over many parts of the equatorial tropics.

In his work to assess the skill of the High Resolution Regional Model in simulation of airflow and rainfall over East Africa, Sakwa (2006), found that the model simulated airflow and precipitation distribution skillfully with some cases and areas of overestimation and underestimation. High rainfall received over parts of East Africa was captured in the model forecast. The results also showed low root mean square errors and mean absolute errors and high correlation coefficients in most parts of the region. The experiments indicated that finer model resolutions produced statistically significant improvements in performance for HRM.

CHAPTER THREE

MODEL APPLIED, DATA AND METHODOLOGY

3.0 INTRODUCTION

This chapter is devoted to the discussion of the model and data used in this study and the various methods used to achieve the objectives of the study..

3.1 Weather Research and Forecasting - Environmental Modeling System

The Weather Research and Forecasting Environmental Modeling System (WRF-EMS) is a complete, full-physics, state-of-the-science Numerical Weather Prediction (NWP) package that incorporates dynamical cores from both the National Center for Atmospheric Research (NCAR) Advanced Research WRF (ARW) and the National Centers for Environmental Predictions' (NCEP) Non-hydrostatic Mesoscale Model (NMM) releases into a single end-to-end forecasting system.

Nearly every element of an operational NWP system has been integrated into the WRF-EMS, including the acquisition and processing of initialization data, model execution, output data processing, and file migration and archiving. Even tools for the display of forecast and simulation data are provided. Real-time forecasting operations are enhanced through the use of an automated process that integrates various fail-over options and the synchronous post processing and distribution of forecast files. A summary of the main features of WRF-EMS are discussed below; more information may be obtained from <http://strc.comet.ucar.edu/wrfems> and the references therein

The main components of the WRF Model are depicted in Figures 2 and 3 respectively. Where the WRF Software Framework (WSF) provides the infrastructure that accommodates multiple dynamics solvers, physics packages that plug into the solvers through a standard physics interface, programs for initialization, and the WRF variational data assimilation (WRF-Var) system. There are two dynamics solvers in the WSF: the Advanced Research WRF (ARW) solver (originally referred to as the Eulerian mass or "em" solver) developed primarily at NCAR, and the NMM (Non-hydrostatic Mesoscale Model) solver developed at NCEP, which is

documented and supported to the community by the Developmental Test bed Center (DTC). While there are multiple solvers, and while not all physics are available to both solvers, the WSF is common to all components. Figure 3 shows a summary of the process flow through the WRF-EMS.

The ARW supports horizontal nesting that allows resolution to be focused over a region of interest by introducing an additional grid (or grids) into the simulation. In the current implementation, only horizontal refinement is available: there is no vertical nesting option. The nested grids are rectangular and are aligned with the parent (coarser) grid within which they are nested.

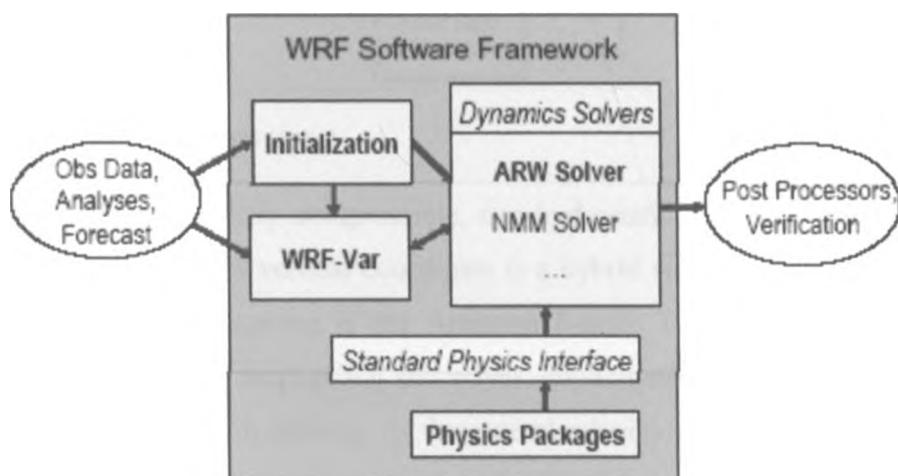


Figure 2: Main Components of WRF-EMS Model

DEPT. OF METEOROLOGY UNIVERSITY OF NAIROBI

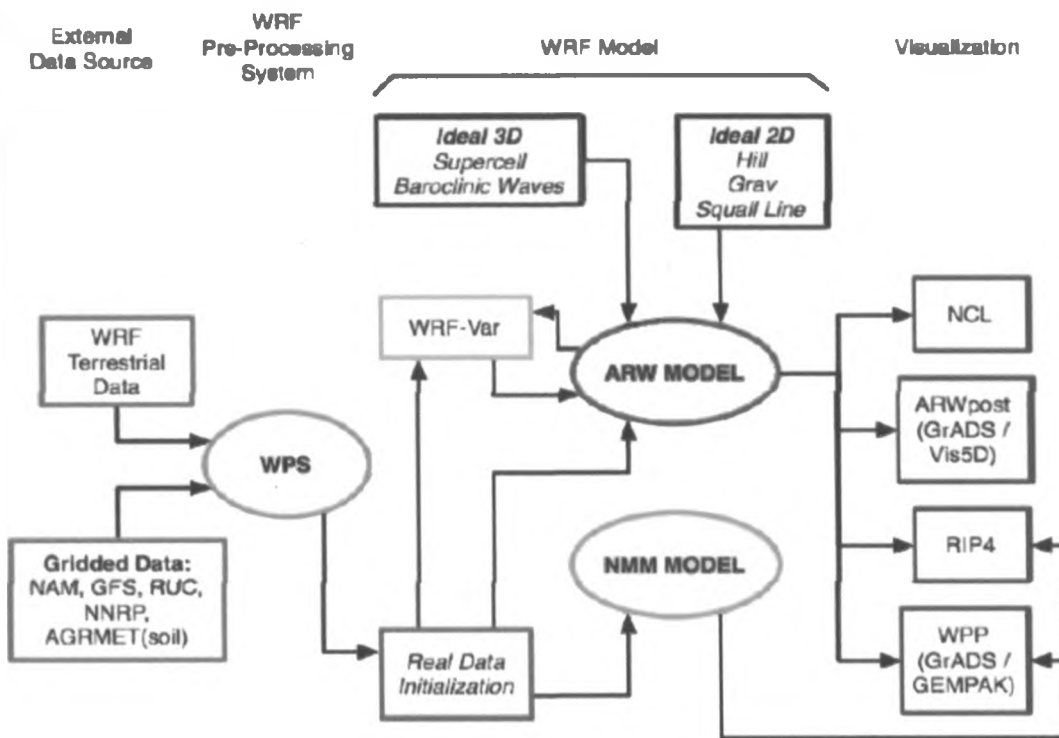


Figure 3: Systems of WRF-EMS Model

The WRF–NMM is a fully compressible, non-hydrostatic mesoscale model with a hydrostatic option (Janjic, 2003). Its vertical coordinate is a hybrid sigma-pressure coordinate as shown in figure 4. The grid staggering is the Arakawa E-grid. The model uses a forward–backward scheme for horizontally propagating fast waves, implicit scheme for vertically propagating sound waves, Adams–Bashforth scheme for horizontal advection, and Crank–Nicholson scheme for vertical advection. The same time-step is used for all terms. The dynamics conserves a number of first and second order quantities, including energy and enstrophy. This model supports a variety of capabilities, including real-data simulations, full physics options, non-hydrostatic and hydrostatic (runtime) options, one-way static nesting and applications ranging from metres to thousands of kilometres.

There are 45 unequally spaced sigma (non-dimensional pressure) levels in the vertical. The physical parameterizations used in this study are Geophysical Fluid Dynamics Laboratory (GFDL) for longwave and shortwave radiation (Lacis and Hansen, 1974; Schwarzkop and Fels, 1991), the Mellor Yamada Janjic (MYJ) scheme for the planetary boundary layer (Janjic, 2002),

the Ferrier scheme for microphysics (Ferrie *et al.*, 2002) and the Janjic Similarity Scheme for the surface layer (Janjic, 1996). The cumulus parameterization used for this study is Grell-Devenyi Cloud Ensemble Scheme: a multi-closure, multi-parameter, ensemble method with typically 144 sub-grid members (Grell and Devenyi, 2002). All the above schemes are well tested for the WRF-EMS system. Table 3 gives a brief illustration of the model configuration in the present study.

The WRF model was configured to solve the following equations:

$$p = \rho R_d T; \dots\dots\dots 1$$

$$\frac{\partial \rho}{\partial t} + \frac{\partial U}{\partial x} + \frac{\partial V}{\partial y} + \frac{\partial W}{\partial z} = 0; \dots\dots\dots 2$$

$$\frac{\partial U}{\partial t} + c_p \Theta \frac{\partial \pi}{\partial x} = -\frac{\partial Uu}{\partial x} - \frac{\partial Vu}{\partial y} - \frac{\partial Wu}{\partial z} + F_x,$$

$$\frac{\partial V}{\partial t} + c_p \Theta \frac{\partial \pi}{\partial y} = -\frac{\partial Uv}{\partial x} - \frac{\partial Vv}{\partial y} - \frac{\partial Wv}{\partial z} + F_y,$$

and

$$\frac{\partial W}{\partial t} + c_p \Theta \frac{\partial \pi}{\partial z} + g\rho = -\frac{\partial Uw}{\partial x} - \frac{\partial Vw}{\partial y} - \frac{\partial Ww}{\partial z} + F_z;$$

.....3

$$\frac{\partial \Theta}{\partial t} + \frac{\partial U\Theta}{\partial x} + \frac{\partial V\Theta}{\partial y} + \frac{\partial W\Theta}{\partial z} = \rho Q. \dots\dots\dots 4$$

The above equations are in cartesian coordinates and neglect the coriolis effect, where, Equation 1 is the Equation of state, Equation 2. is the equation of Conservation of mass, Equation 3. is the equation of Conservation of momentum and finally Equation 4. Is the 'equation for Conservation

of energy. In those equations, (v, w) are the velocity components in the (x, y, z) directions, θ is the potential temperature, and ρ is the air density.

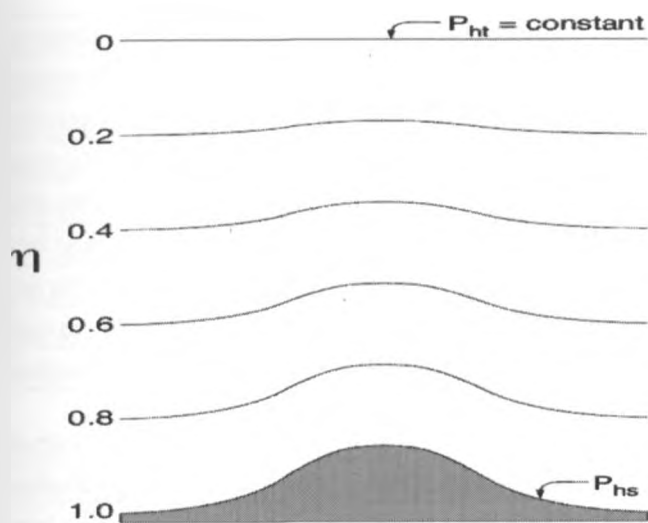


Figure 4: WRF vertical coordinate

3.2 Experimental Design

In the present simulation, the model was integrated for a period of 90 days, starting at 0000 UTC of 1st March to 31st May of 2011. A single domain with 14 km spatial resolution was configured. Initial conditions for the 14 km domain are derived from 6 h GFS Global Analyses at $1.0^\circ \times 1.0^\circ$ grids. Analysis fields, including temperature, moisture, geopotential height and wind, are interpolated to the mesoscale grids by the WRF preprocessing system (WPS). These derived fields are used as initial conditions for the present experiments. The experimental domain is $26.0\text{--}51.0^\circ\text{E}$ and $12.0^\circ\text{S}\text{--}12.0^\circ\text{N}$. With a horizontal grid ranging from the Eastern Atlantic to western Indian Ocean, all domains are centered over Kenya to represent the regional-scale circulations and to resolve the complex flows in this region.

For the microphysics scheme, Lin *et al.* scheme was used which is a sophisticated scheme that has ice, snow and graupel processes, suitable for real-data high-resolution simulations. Kain-

Fritsch scheme which is a cumulus scheme was used, and it is Deep and shallow convection sub-grid scheme using a mass flux approach with downdrafts and CAPE removal time scale.

Table 1: WRF-EMS model physics and dynamics configurations

Dynamics	Non-hydrostatic
Model domain	12.0°S–12.0°N, 26.0–51.0°E
Primary Time Step	80 Seconds
Vertical Layers	45
Grid Dimension	202 × 171
Grid Spacing	14 km
Top of Model Atmosphere	50 mb
Map projection	Rotated latitude and longitude
Horizontal grid system	Arakawa E-grid
Vertical coordinate	Terrain-following hybrid (sigma-pressure) vertical coordinate (38 sigma levels)
Radiation parameterization	GFDL/GFDL
Land surface	Noah Land Surface Model
Surface layer Physics	Monin-Obukhov
Cumulus Scheme	Kain-Fritsch
PBL Scheme	Yonsei University scheme
Microphysics Scheme	Lin et al. scheme, for high spatial resolution

3.3 Data

The data used in this study include observed rainfall and temperature from Kenya Meteorological Department and boundary data which constitute the initialization data for the WRF-EMS model was obtained from the Global Forecasting Model.

3.3.1 Rainfall and Temperature data

The daily observed data for rainfall and temperature for Kenya for the period March, April and May 2011 were used in this study and these data were obtained from the Kenya Meteorological Department. A total of 27 stations were used in the study as shown in Figure 4.

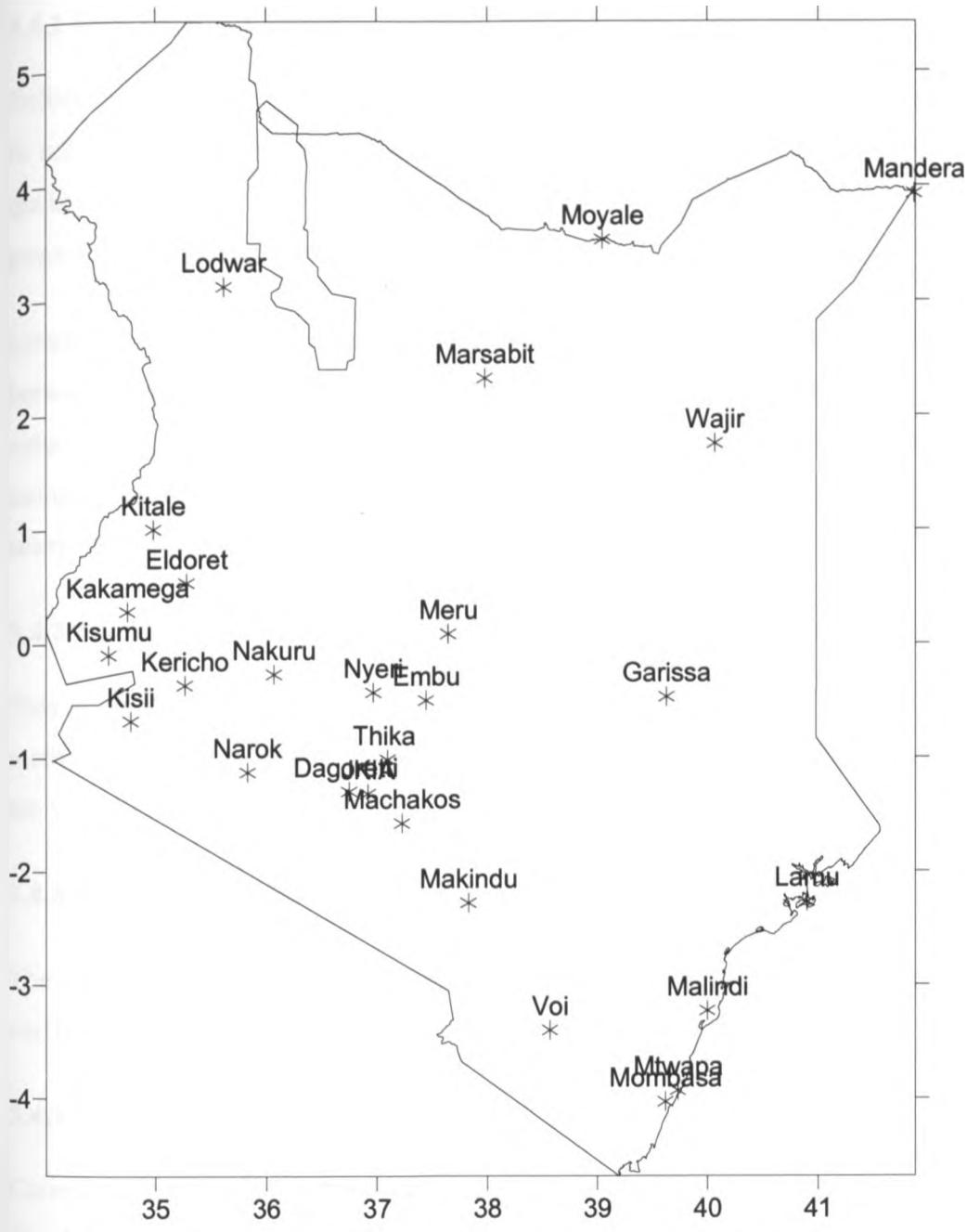


Figure 5: Study area showing the location of stations used in the analysis

3.4 METHODOLOGY

This section presents methods that were used in this study they include; data quality control, graphical presentation, correlation analysis, Absolute Mean Error (AME), Root Mean Square Error (RMSE), Frequency Bias Index (FBI), Equitable Threat Score (ETS), and True Skill Statistic (TSS) and Percentage correct (PC)

3.4.1 Data Quality Control

Before the analysis could be done on the data, there was a need for data quality checks. In order to make valid inferences from analysis of the observed data, it was necessary to ascertain the quality of the data. An error in the data arises from station conditions, coding and decoding procedures, instruments and human error.

Linear regression was used to fill in the missing data. Simple correlation calculations were made between stations close to each other geographically. From the correlation analysis the missing value was estimated using the station that had the highest correlation and that had a value in that month. Mass and double mass curves were used to assess the quality of the estimated data in this study. 9% of the data were estimated in all locations.

3.4.2 Assessment of the Spatial Distribution of Observed and Simulated Data

This involves the graphical display and time series analysis of rainfall and temperature data. The method was used to determine the performance of rainfall during the March to May season for the year 2011.

3.4.3 Verification of the Model Out put

The verification of the model output was done using analysis of errors, correlation analysis and verification skill scores.

3.4.3.1 Correlation Analysis

Correlation analysis provides the degree of linear association between a pair of variables. The simple correlation coefficient (r) between a model output variable (F) and the corresponding observation (O) is given by:

$$r = \frac{\sum_{i=1}^M (O - \bar{O})(F - \bar{F})}{\sqrt{\sum_{i=1}^M (O - \bar{O}) \sum_{i=1}^M (F - \bar{F})}} \dots\dots\dots(5)$$

In Equation 5, \bar{O} and \bar{F} are sample means of observed data and model outputs, respectively, and M is the total number of cases used in the analysis. The symbol r indicates the correlation of the forecast to the observation; a high (low) r value indicates higher (lower) correlation between the two

3.4.3.2 Root Mean Square Error and Absolute Mean Error (AME)

Root mean square error is a frequently used measure for computing the differences between values predicted by a model and the actual observations. Equation 6 is the formula for computing the RMSE while equation 7 is used to compute the AME.

$$RMSE = \sqrt{\frac{\sum_{i=1}^M (F_i - O_i)^2}{N}} \dots\dots\dots 6$$

In Equations 6 and 7, F_i and O_i are the model simulated and observed values, respectively, N is the total number of observation or forecast.

$$AME = \sum_{i=1}^M \frac{|F_i - O_i|}{N} \dots\dots\dots 7$$

3.4.3.3 Verification scores

In this study, categorical statistics were used to analyse the relationship between the model outputs and the observed rainfall values. The scores were evaluated using a 2 by 2 contingency table. Table 2, displays the basic structure and entries from the categorical analysis from which some skill scores were determined for different thresholds, they include 0.1, 0.5, 1.0, 3. 5 and 10mm. Skill scores are measures of skill and those used in this study are briefly described below.

Table 2: A 2 by 2 Contingency Table

	Observed yes	Observed no	Total
Forecasted yes	A	B	E
Forecasted no	C	D	F
Total	G	H	T

In Table 2, A is the number of correct forecasts, B is the number of incorrectly forecasts, C is the number of forecasts failing to predict an observed event and D is the number of correct negative forecasts. The scores that were evaluated to determine the skill of the model are; Frequency Bias Index (FBI), Equitable Threat Score (ETS), and True Skill Statistic (TSS) and Percentage correct (PC)

$$FBI = \frac{A+B}{A+C} \dots\dots\dots 8$$

and

$$ETS = \frac{A - R(A)}{A+B+C - R(A)} \dots\dots\dots 9$$

$$R(A) = \frac{(A+B)(A+C)}{A+B+C+D} \dots\dots\dots 10$$

And

$$TSS = \frac{AD - BC}{(A+C)(B+D)} \dots\dots\dots 11$$

$$PC = \frac{A+D}{T} \dots\dots\dots 12$$

FBI measures the event frequency with no regard to the accuracy. Its value is 1 for a perfect forecast, and it is larger (smaller) than 1 if the system is over forecasting (under forecasting). The

ETS is a modified version of the threat score rendered equitable by taking subtracting a random forecast ($R(A)$). Therefore, a chance forecast will score 0, as will a constant forecast. A perfect forecast will have an ETS equal to 1. As in the ETS, also the TSS receives 0 for random and constant forecasts. While a higher score is obtained if a rare event is forecasted correctly.

CHAPTER FOUR

RESULTS AND DISCUSSIONS

4.0 INTRODUCTION

In this chapter, the results are presented and discussed, starting with the performance of the observed March–May 2011 seasonal rainfall, observed and forecasted spatial distribution of the rainfall and temperature during the March-May 2011 season, and finally the results from assessment of the model accuracy and skill.

4.1 The Performance of the Rainfall during March-May 2011 Season

Figure 6 and 7 shows that March to May 2011 seasonal rainfall for most parts of the country was highly depressed and poorly distributed, both in time and space, over most parts of the country. This was more so over the North-eastern parts of Kenya and the Coastal strip where most meteorological stations recorded less than 50 percent of their seasonal Long-Term Means (LTMs) during March to May season Mombasa, Garissa, Lamu, Wajir, Moyale and Marsabit stations recorded less than 40% of their seasonal LTMs. The rainfall was also characterised by late onset in some parts of the country. A few stations namely Kitale, Embu, Machakos, Kisii, Lodwar, Nakuru, Voi, Kericho and Kakamega, however, recorded rainfall that was within the near-normal category (between 75 and 125% of their seasonal LTMs) but the distribution was also generally poor with a prolonged dry spell in April.

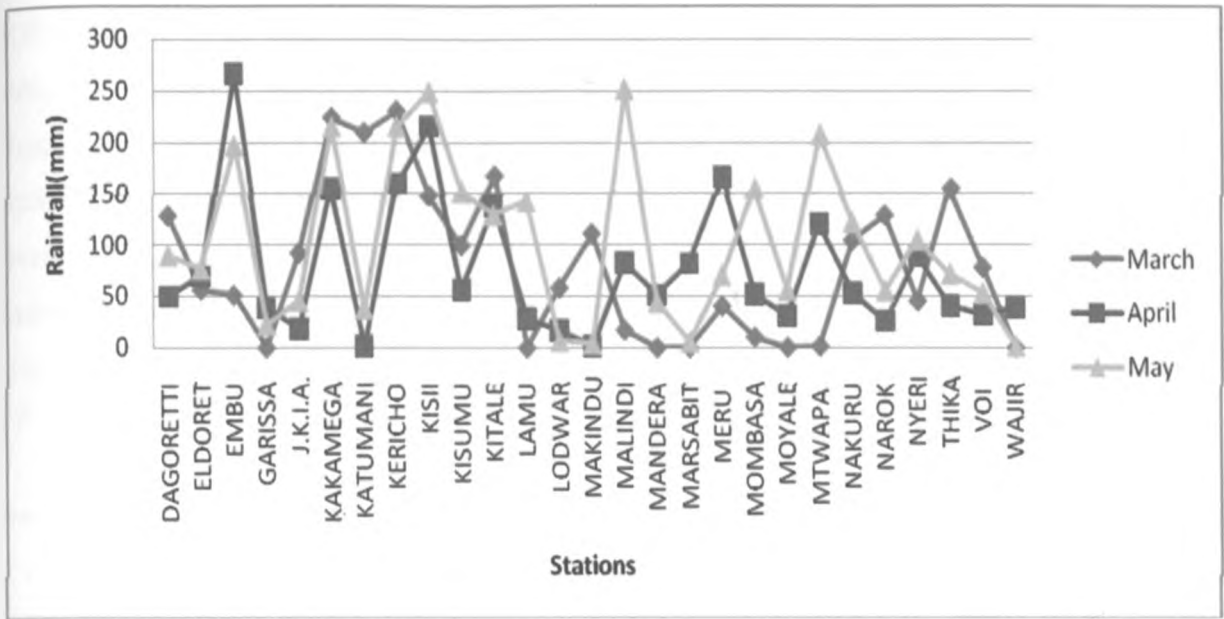


Figure 6: The rainfall performance of March-May 2011 season

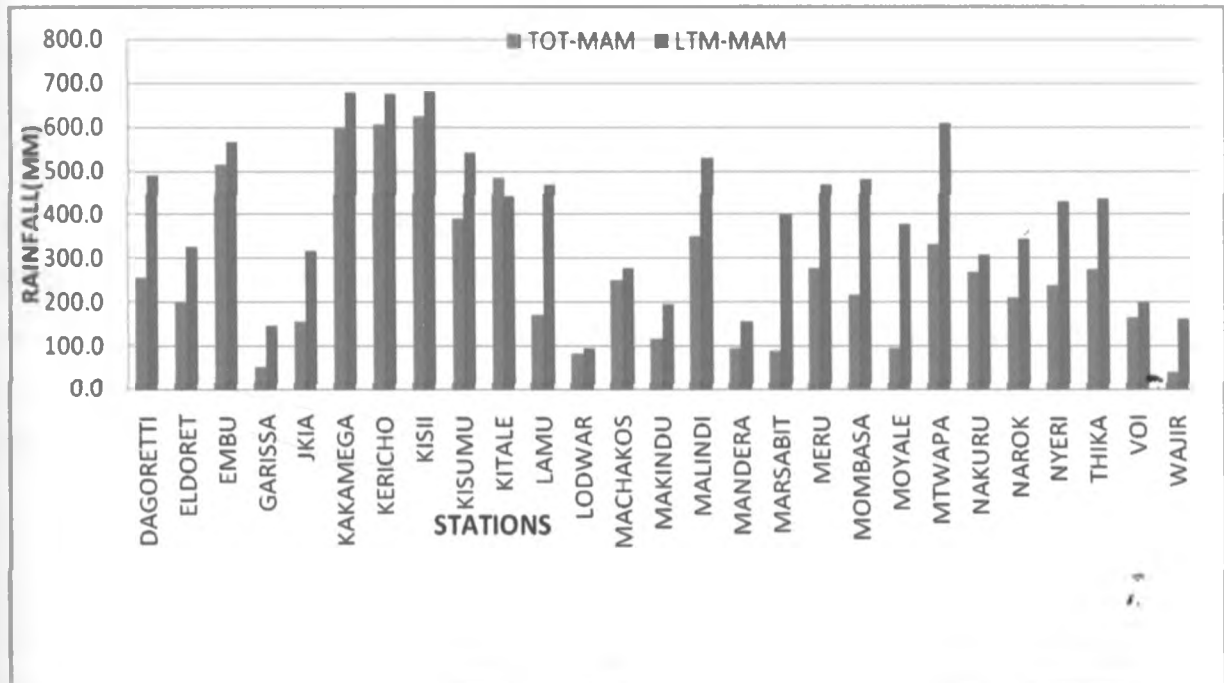


Figure 7: The rainfall performance of March-May 2011 season

Although the seasonal rainfall was characterized by long dry spells and low rainfall values in different parts of the country especially in April, a few rainfall storms were recorded during the period. The heaviest storm of 101.5 mm was recorded at Embu station on 27th of April 2011. The same station recorded 57.3 and 76.6 mm on 4th and 7th of May 2011 respectively. The second heaviest storm amounting to 100.6 mm was recorded at Machakos station on 18th of March. The same station recorded 62.2 mm the following day (19th of March). Other rainfall storms recorded during the season include 73.9 mm and 91.5 mm recorded at Voi and Kisumu on 24th and 31st of March 2011 respectively, and 55.3 and 60.4 mm recorded at Meru and Kakamega on 21st and 30th of April 2011 respectively.

For the entire season, Kisii meteorological station recorded the highest rainfall amount of 611.8mm, which was 91.7% of the LTM. Kericho, Kakamega, Embu, Kitale, Kisumu, Meru, Thika, Nakuru, Dagoretti Corner and Mtwapa stations recorded 605.4mm (79%), 594mm (78%), 513.8mm (90%), 482.3mm (109%), 388.7mm (71.8%), 276.4mm (59%), 274.6mm (63%), 268.6mm (87.1%), 267.3mm (53%) and 330.2mm (54.4%) respectively. The rest of the station recorded less than 250mm as shown in Table 3.

The rainfall during the month of March, April and May 2011 season, was depressed, because of the prevailing cooler than average Sea Surface Temperatures (SSTs) over the Eastern and Central Equatorial Pacific Ocean, indicating that the moderate La Niña conditions still prevailed in the Pacific. Cooler than average SSTs also occurred in the SW Equatorial Indian Ocean adjacent to the East African Coastline. These temperature patterns weakened the rainfall generating mechanism that led to depressed rainfall over most parts of the country. The zonal arm of the rain-bearing system, the ITCZ, was generally diffuse and mainly overlying northern Tanzania for most of the period.

From the figure 8 it can be seen that, during the month of March the winds were generally northeasterly, while in figure 9 shows that in May the winds were southeasterly. Therefore, it can be seen that the month of March was mainly influenced by continental dry winds from Arabian high while during the month of May which received heavy rains was due to the southeasterly winds which was maritime.

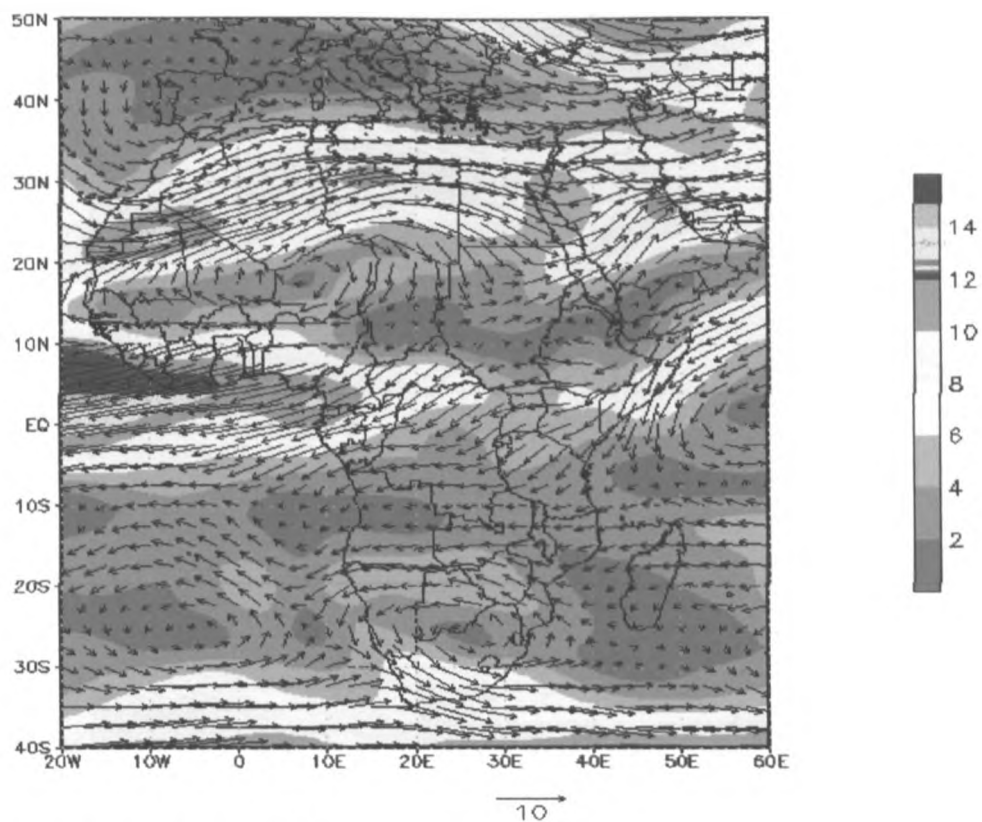


Figure 8: the general circulation for March, 2011 at 700mb level

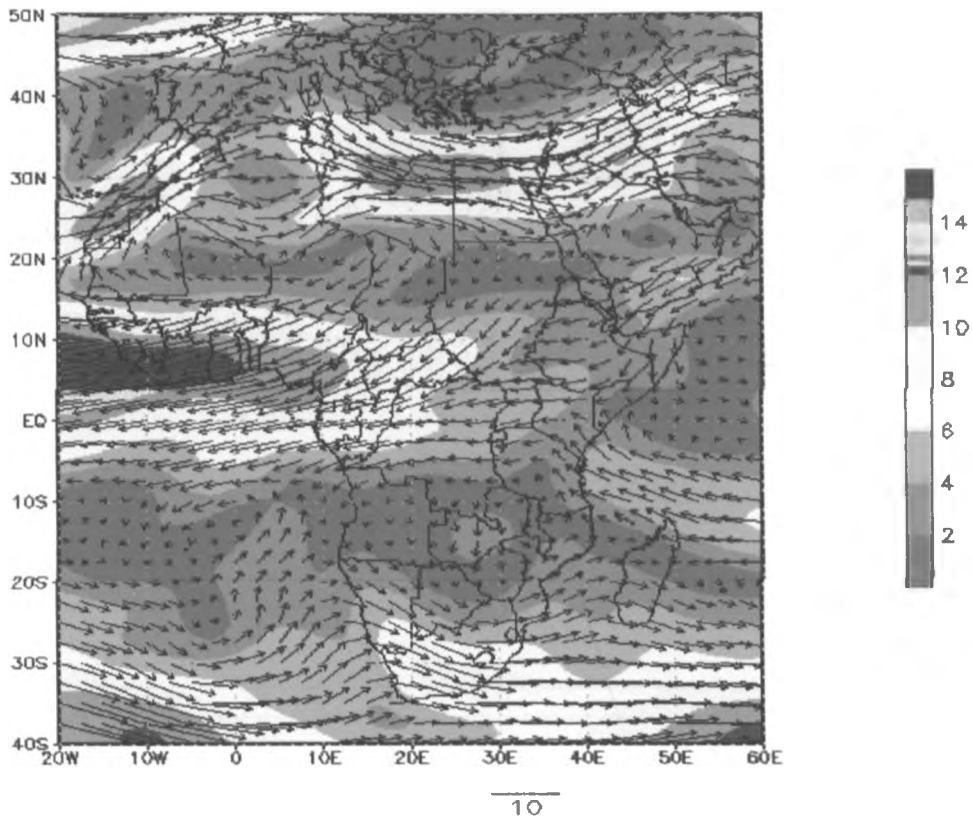


Figure 9: the general circulation for May, 2011 at 700mb level

4.2 Spatial Distribution of Observed and Forecasted Rainfall and Temperature

This section presents the results from spatial distribution analysis of the observed and the forecasted rainfall and temperature. From Figure 10, 11, 12 and 13 it is evident that the spatial pattern of the rainfall simulated by WRF-EMS model was similar to the observed, except for some few stations where the model either under estimated or over estimated.

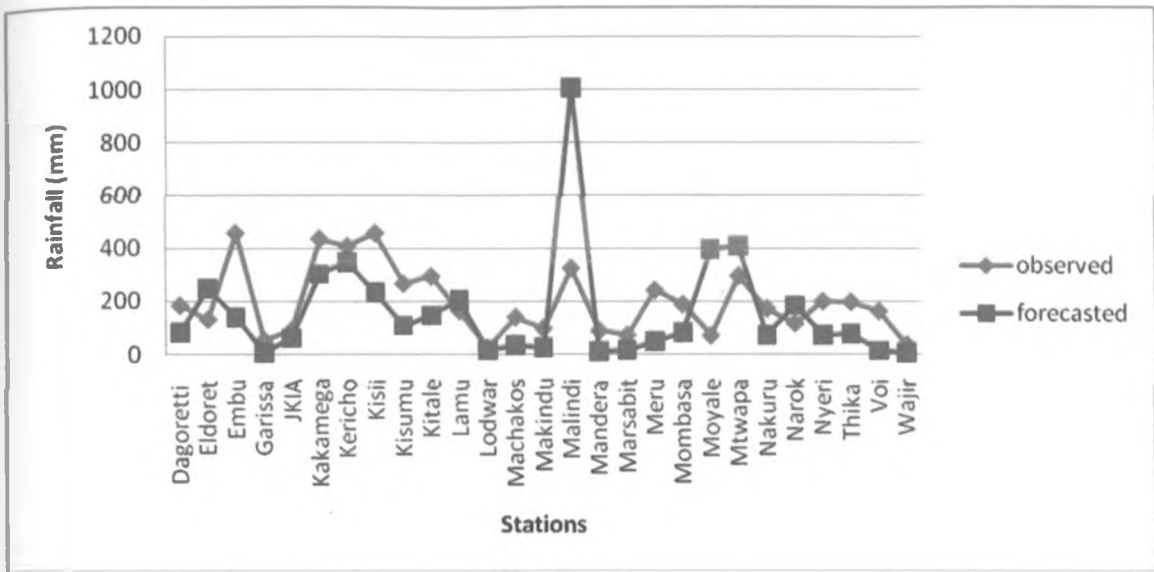


Figure 10: The observed and forecasted rainfall for the March-May 2011 season

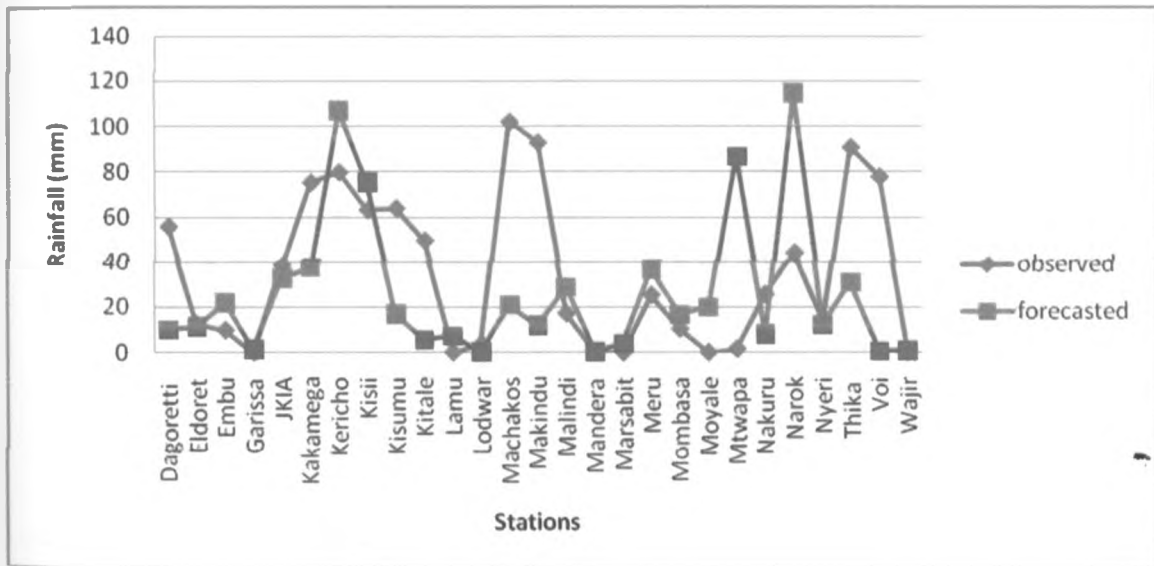


Figure 11: The Observed and Forecasted rainfall for the month of March 2011

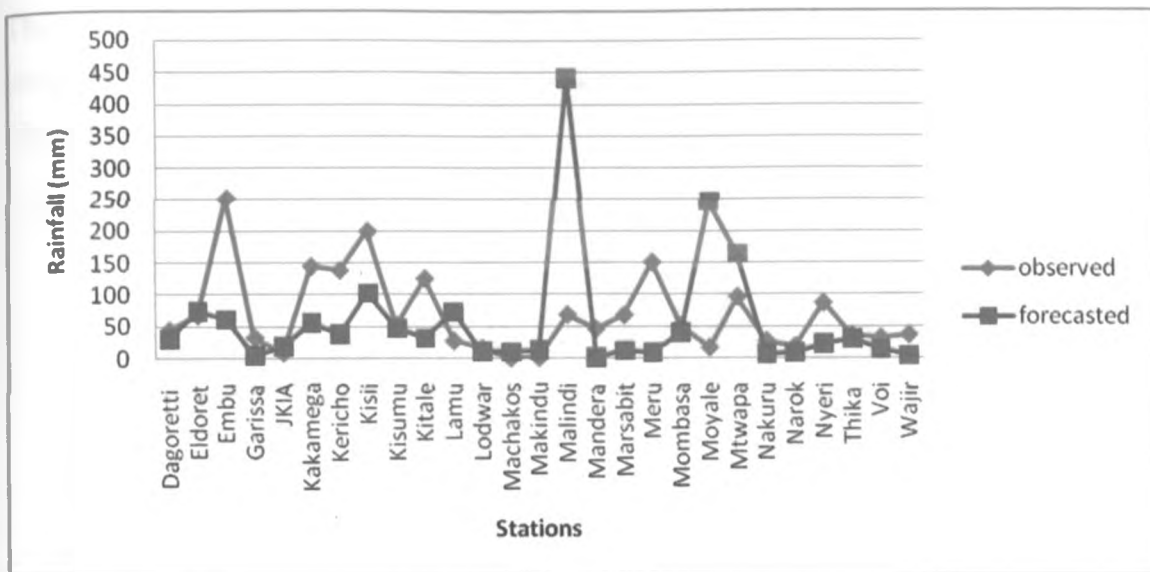


Figure 12: The Observed and Forecasted rainfall for the month of April 2011

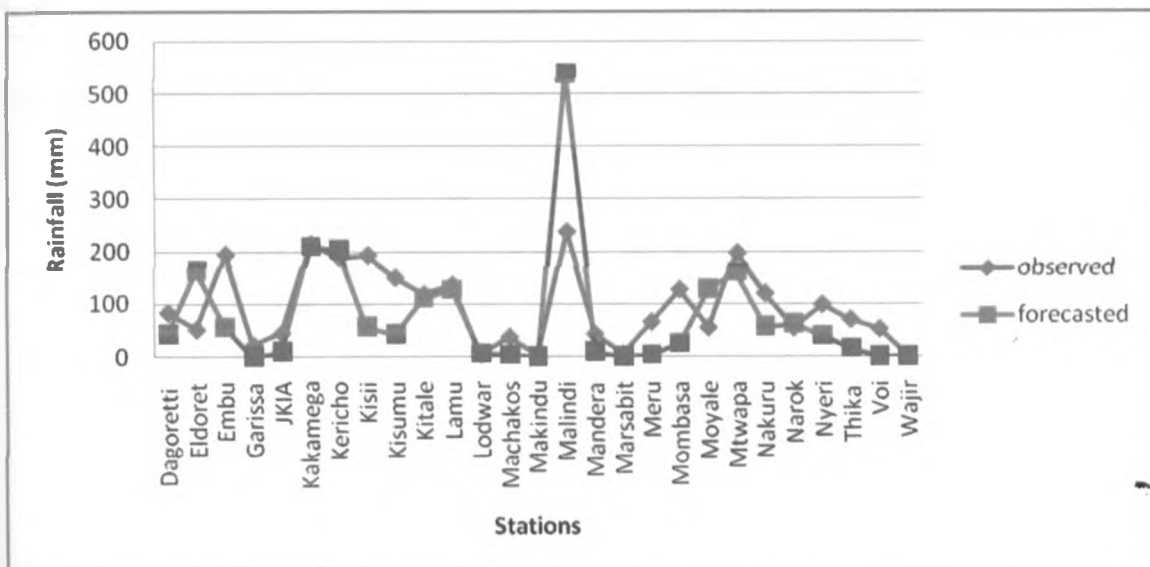


Figure 13: Observed and Forecasted rainfall for the month of May 2011

The results from the temperature analysis shows that the model simulated well the observed temperature over most stations for the whole season of March to May, as shown in Figure 14, 15, 16, and 17.

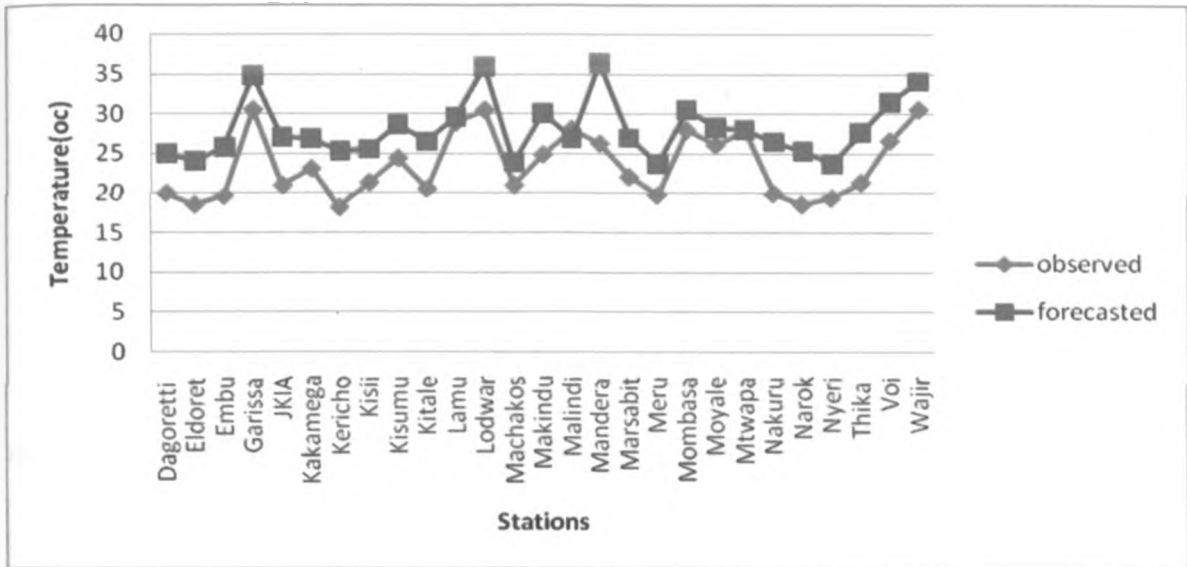


Figure 14: The observed and forecasted temperature for March-May 2011 season

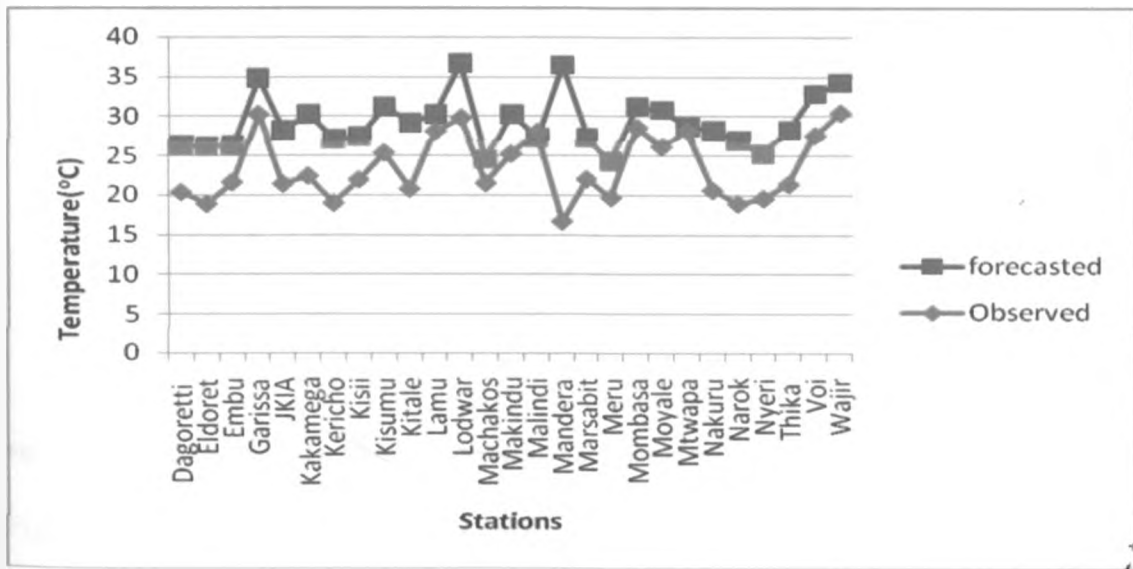


Figure 15: The observed and forecasted temperature for the month of March 2011

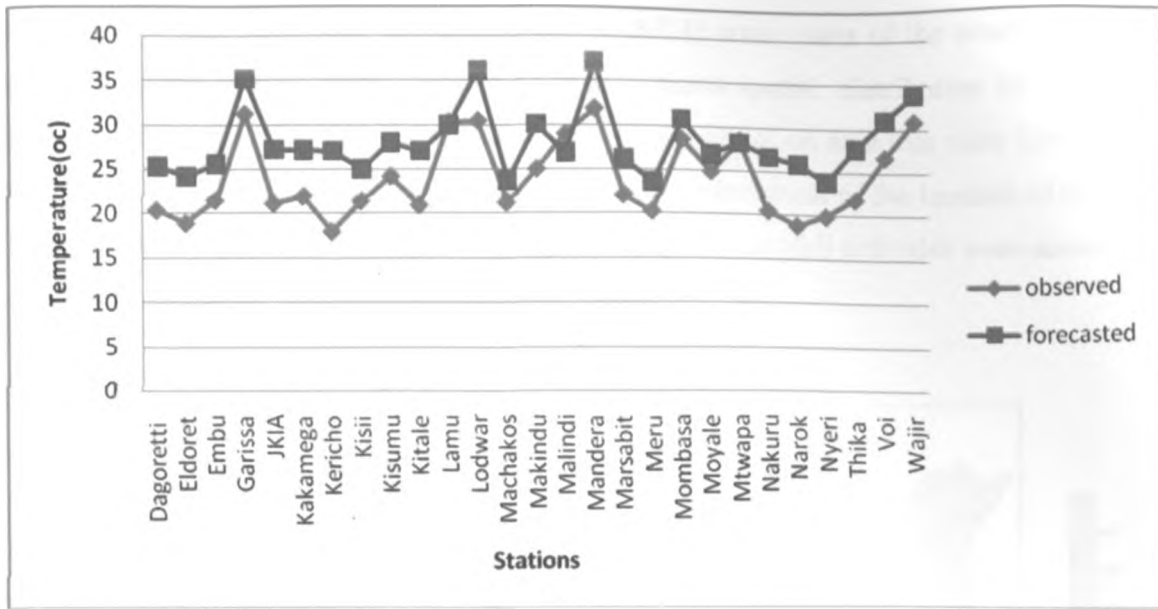


Figure 16: The observed and forecasted temperature for the month of April 2011

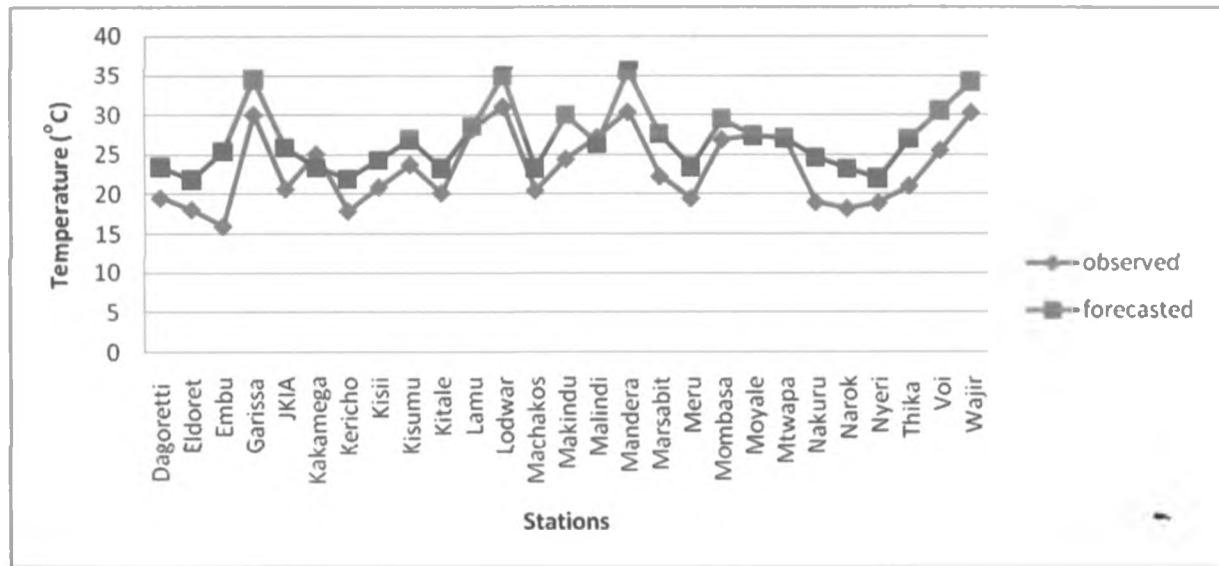


Figure 47: The observed and forecasted temperature for the month of May 2011

Figures 18, 19, 20 and 21 shows the spatial distribution for the MAM season, In those figures, its evident that the model was able to simulate the general pattern of the spatial rainfall distribution, it however failed to capture the fine details as it can be seen in figure 18 where the model over estimated the rainfall over the the coast and underestimated the rains over the Lake Victoria region. This shows the deficiency in the model to reproduce the effects of small scale

systems that may have been responsible for rainfall in some parts of the country during some days within the season. From Figures 22 and 23 shows spatial distribution for March 6th and May 1st shows that that the model was able to give a signal on area that were likely to receive high rainfall in those days, although their was some displacement of the location of the observed heavy rainfall. The result shows that during some days the rainfall activities were associated with the system that were well represented by the model.

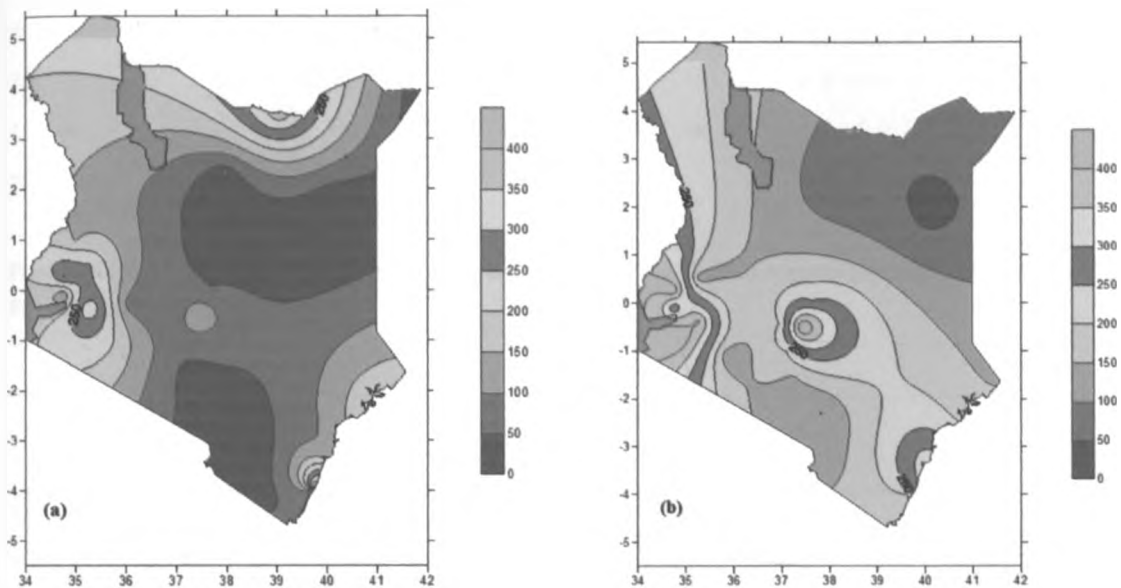


Figure 18: spatial distribution of Rainfall for the March-May 2011 season (a) Observed Rainfall (b) Forecasted Rainfall

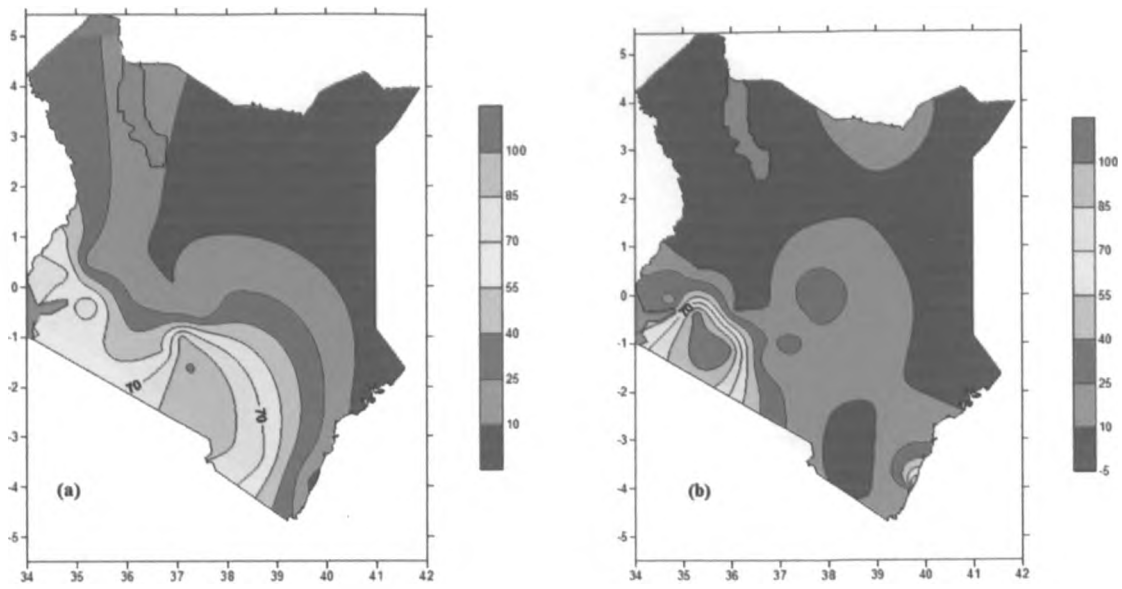


Figure 59: Spatial distribution of Rainfall for the month of March 2011 season (a) Observed Rainfall (b) Forecasted Rainfall

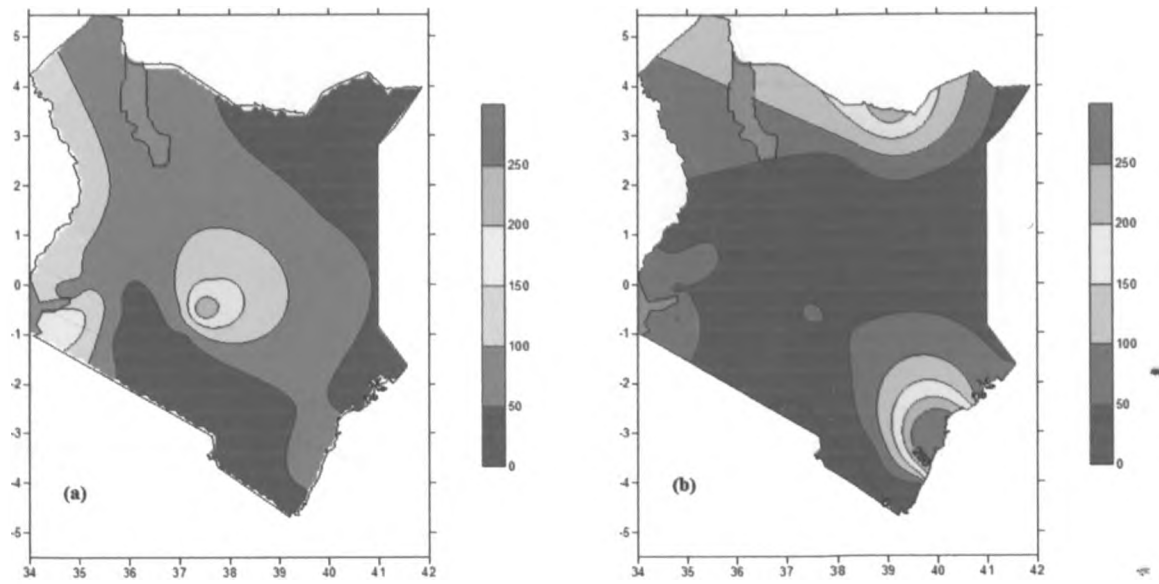


Figure 20: Spatial distribution of Rainfall for the month of April 2011 season (a) observed Rainfall (b) Forecasted Rainfall

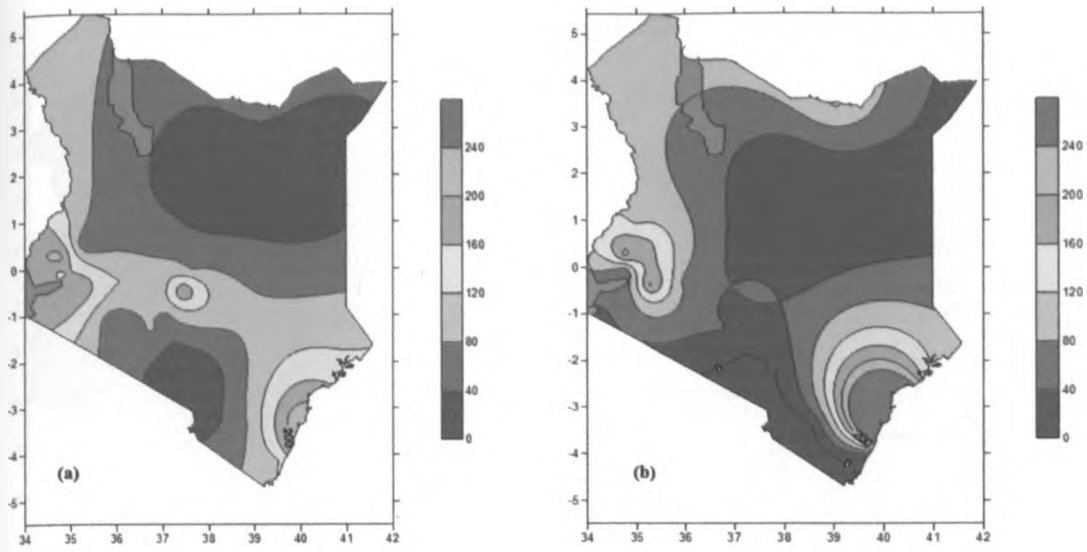


Figure 21: Spatial distribution of Rainfall for the month of May 2011 season (a) observed Rainfall (b) Forecasted Rainfall

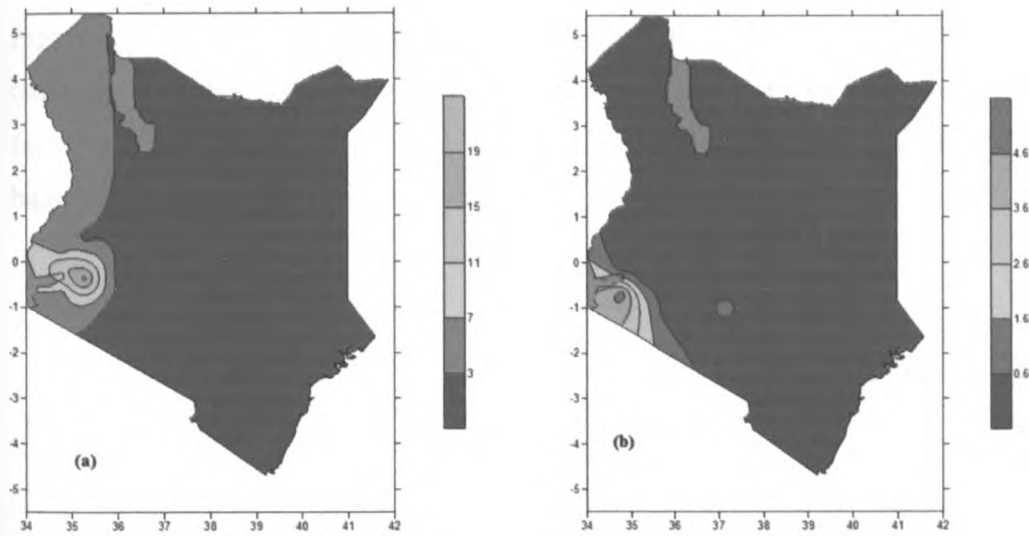


Figure 22: Spatial Distribution of Rainfall for March 6th 2011 (a) Observed (b) Forecasted

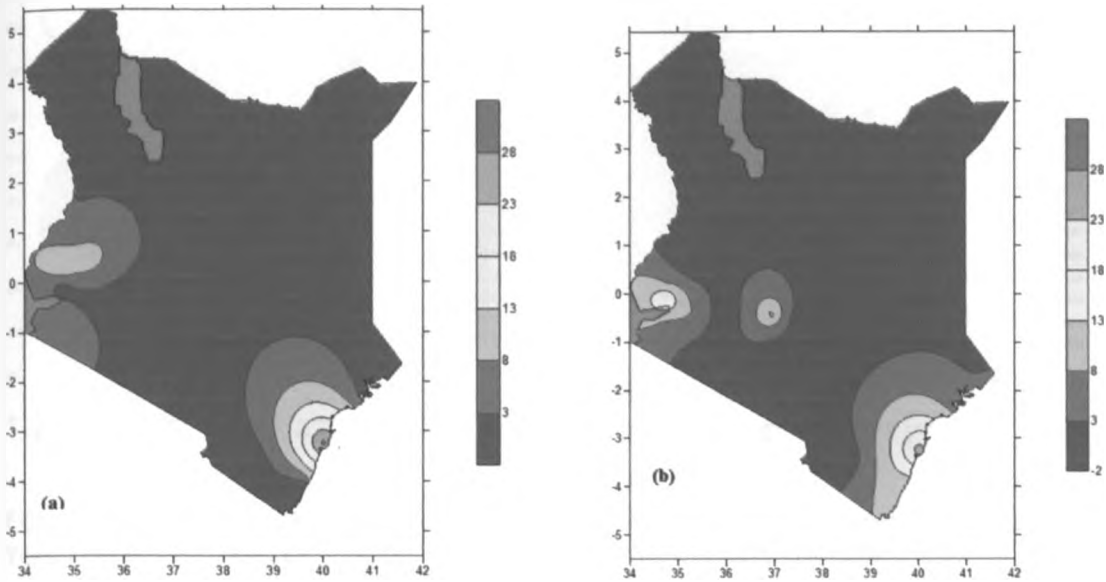


Figure 63: Spatial Distribution of Rainfall for May 1st 2011 (a) Observed rainfall (b) Forecasted rainfall

Figures 24, 25 and 26 shows that the model simulated well the observed spatial distribution of temperature, although in most cases it overestimated the observed temperature. This is due to the fact that unlike rainfall, temperature is a continuous field and determined largely by the radiative balance that is well represented by the model.

DEPT. OF METEOROLOGY UNIVERSITY
OF NAIROBI

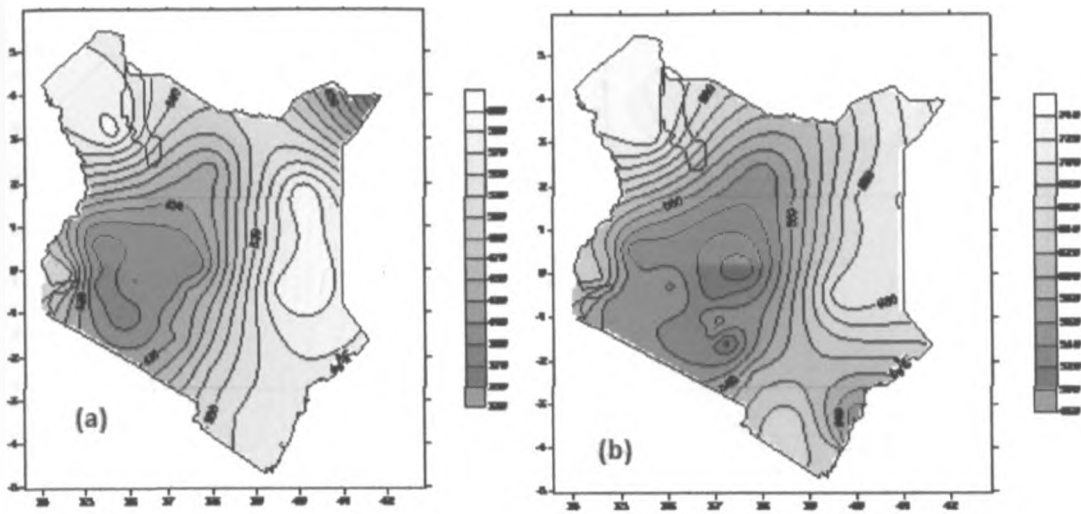


Figure 74: Spatial Distribution of temperature for March 2011 (a) Observed temperature (b) Forecasted Temperature

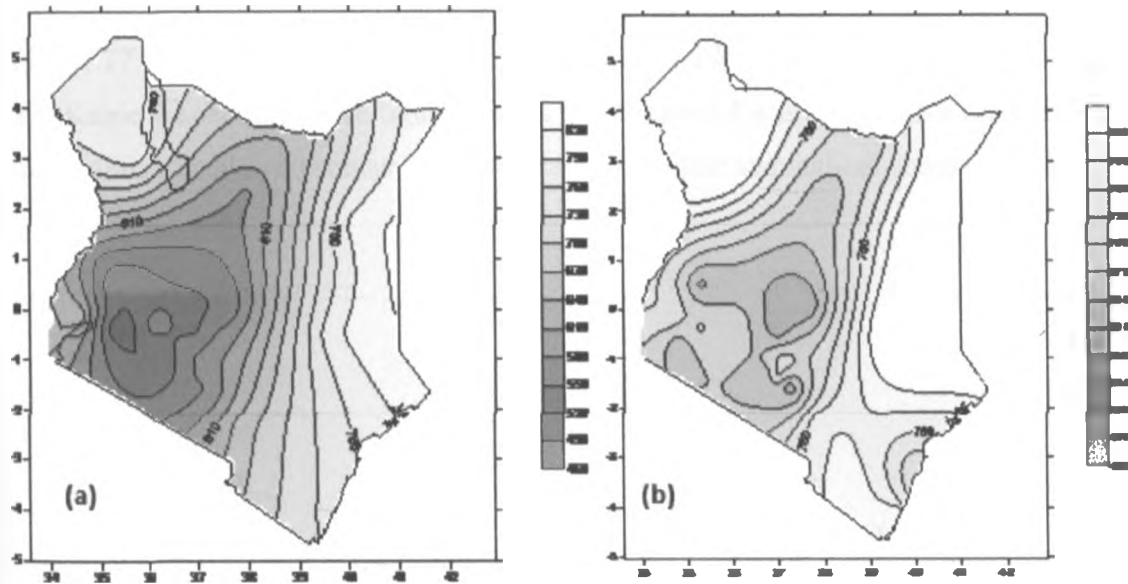


Figure 85: Spatial distribution of temperature for April 2011 (a) Observed temperature (b) Forecasted temperature

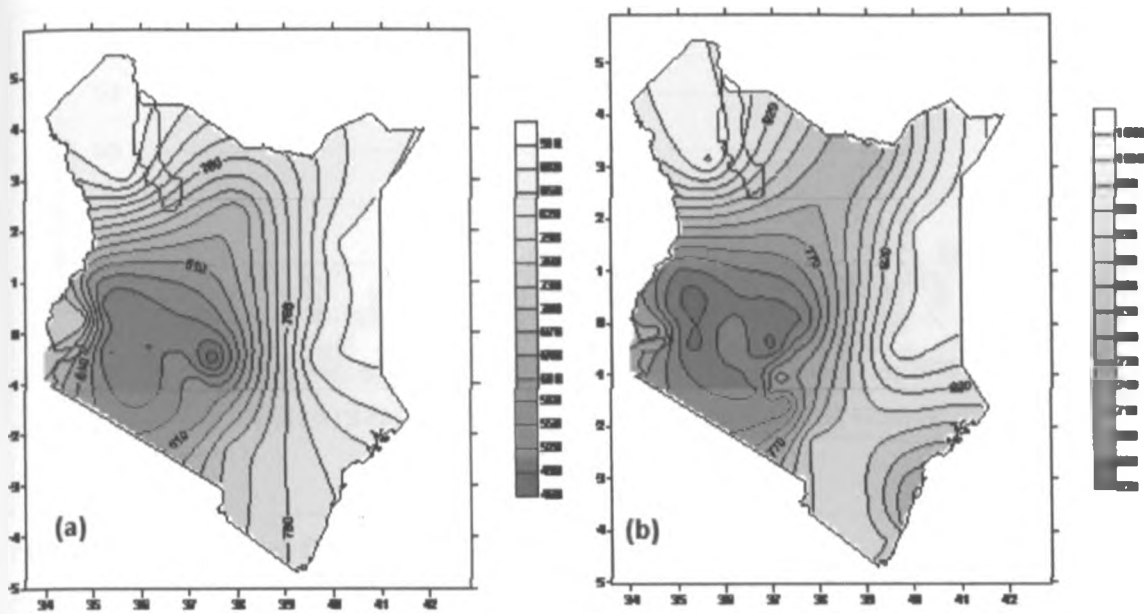


Figure 26: Spatial distribution of temperature for May 2011 (a) Observed temperature (b) Forecasted temperature

Figure 27 and 28 shows the time series for both observed and forecasted rainfall over Malindi and Kitale Respectively. The figures shows that the model was able to give the right signal but it underestimated and overestimated in some days for Kitale and malindi stations respectively.

DEPT. OF METEOROLOGY UNIVERSITY
OF NAIROBI

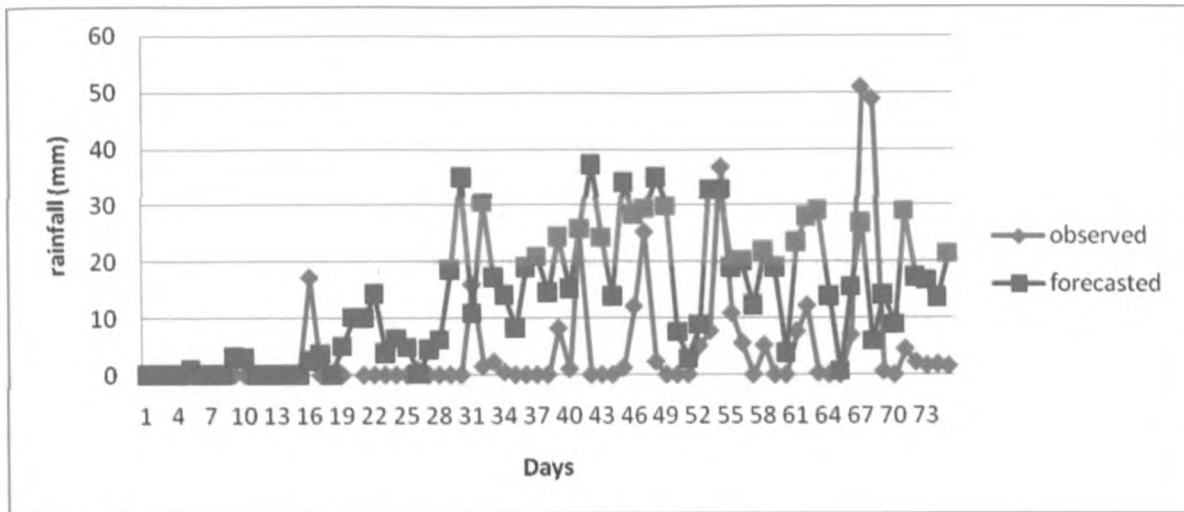


Figure 27: Time series for MAM, 2011 season for Malindi station

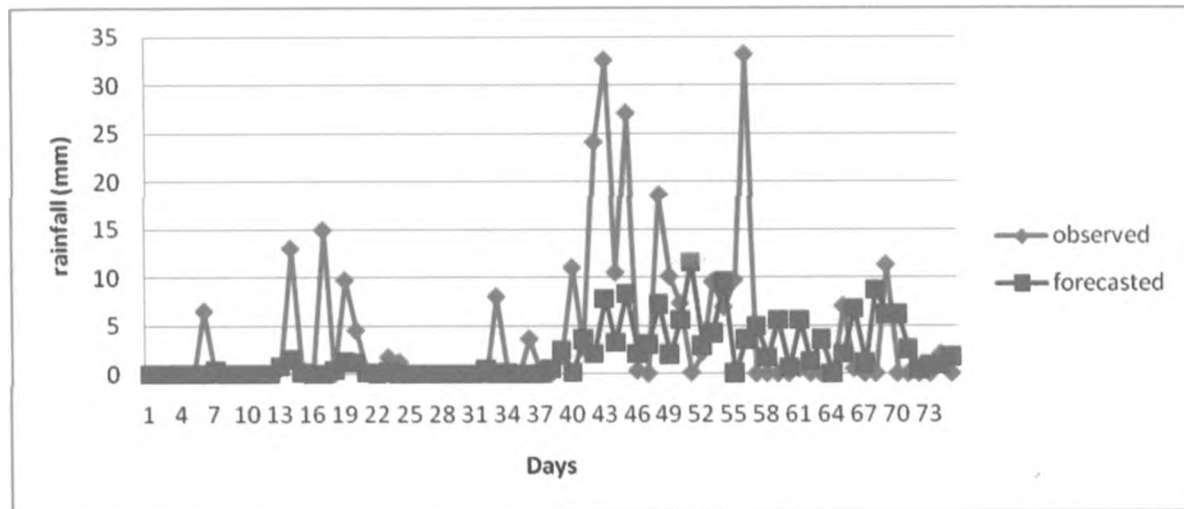


Figure 28: Time series for MAM, 2011 season for Kitale station

4.3. Results from Assessment of Model Accuracy and Skill

This section presents the results from the various methods that were used to assess model skills and accuracy. The accuracy was assessed by using Root Mean Square Error (RMSE), Absolute Mean error (AME) and correlation coefficient. While the skill was determined using categorical statistics that included, Frequency Bias Index, True Skill Statistics, Equitable Threat Scores and percentage correct.

4.3.1 Results From the Analysis of the Model Accuracy

Correlation coefficient (CC), Absolute mean error (AME) and Root mean square error (RMSE) were calculated between the observed and the model output for both rainfall and temperature. Tables 4 and 5 shows the results for CC, AME and RMSE for March to May 2011.

The results from correlation coefficient analysis shows that the number of stations with high correlation is highest in March and lowest in April. April is the peak rainfall month, and it is a month when the contribution of rainfall from meso-scale system is highest. In March most region were dry and rainfall was caused mainly by large scale systems. Most of the stations had a positive coefficient but some of the stations had negative correlation indicating an inverse-relationship between the observed rainfall and temperature and the model output for the months of March, April and May. However the correlation coefficient for temperature had more station with positive coefficients as compared to that of Rainfall as shown in Tables 4 and 5.

From the results in Tables 4 and 5 the Absolute mean error for most station was less than 10, indicating that the model had a high accuracy in reproducing the observed precipitation and temperature. Also the results shows a very low RMSE of less than 10 for all stations, this indicate the ability of the model to reproduce the observed temperature and rainfall.

DEPT. OF METEOROLOGY UNIVERSITY
OF NAIROBI

Table 3: Correlation Coefficient (CC), Absolute Mean Error (AME) and Root Mean Square Error (RMSE) for Rainfall for March, April and May

Months	March			April			May		
Name of station	CC	AME	RMSE	CC	AME	RMSE	CC	AME	RMSE
Dagoretti	0.69	2.30	9.37	-0.02	0.58	5.01	0.22	4.30	5.37
Eldoret	0.50	0.06	1.92	0.46	0.23	7.01	0.36	3.84	3.04
Embu	0.62	0.60	1.57	0.12	7.31	20.93	-0.04	4.78	4.24
Garissa	0.00	0.07	0.27	-0.11	1.12	3.78	-0.05	0.76	2.03
JKIA	0.91	0.29	3.12	-0.10	0.35	2.12	0.16	1.22	2.39
Kakamega	0.92	1.90	3.83	0.08	3.39	13.83	0.38	0.16	3.11
Kericho	0.54	1.34	4.43	-0.12	3.87	9.42	0.27	0.48	2.88
Kisii	0.48	0.60	7.79	-0.09	3.74	18.92	0.43	4.71	2.96
Kisumu	0.35	2.36	5.81	0.16	0.18	5.44	-0.08	3.71	3.03
Kitale	0.52	2.22	4.90	0.82	3.62	8.09	0.10	0.29	2.75
Lamu	0.00	0.36	0.85	0.56	1.74	4.06	0.06	0.36	2.73
Lodwar	-0.06	0.18	0.81	0.11	0.25	3.38	-0.02	0.03	1.11
Machakos	0.83	4.08	12.26	-0.02	0.32	1.11	0.59	1.17	1.99
Makindu	0.58	4.06	12.79	-0.06	0.43	0.99	-0.07	0.14	0.79
Malindi	0.23	0.57	4.36	0.22	14.35	17.89	0.23	10.35	4.27
Mandera	0.00	0.01	0.03	-0.08	1.78	7.03	-0.04	1.16	2.32
Marsabit	0.00	0.19	0.45	-0.05	2.17	7.66	-0.06	0.16	0.92
Meru	0.89	0.56	2.45	0.05	5.46	14.17	0.02	2.13	2.47
Mombasa	-0.20	0.31	2.90	0.05	0.44	4.96	0.45	3.53	2.84
Moyale	0.00	0.99	2.15	0.30	8.83	12.67	0.37	2.51	2.79
Mtwapa	-0.11	4.25	7.63	-0.02	2.60	10.58	0.67	1.29	3.13

Nakuru	0.91	0.90	3.06	-0.10	0.78	2.28	0.45	2.17	2.57
Narok	0.68	3.52	20.34	0.04	0.38	2.19	0.01	0.24	3.28
Nyeri	0.78	0.10	1.92	-0.01	2.49	5.89	-0.03	2.06	2.64
Thika	0.79	3.01	11.90	0.02	0.25	4.18	0.23	1.88	2.68
Voi	-0.05	3.88	16.54	0.06	0.72	3.68	-0.06	1.81	2.55
Wajir	0.00	0.04	0.16	0.04	1.28	3.86	-0.06	0.01	0.46

DEPT. OF METEOROLOGY UNIVERSITY
OF NAIROBI

Table 4: Correlation Coefficient (CC), Absolute Mean Error (AME) and Root Mean Square Error (RMSE) for Temperature for March, April and May

Months	March			April			May		
NAME	CC	AME	RMSE	CC	AME	RMSE	CC	AME	RMSE
Dagoretti	0.12	6.04	6.15	0.38	4.97	5.043	0.10	3.91	4.13
Eldoret	0.33	7.29	7.42	-0.08	5.42	6.369	-0.01	3.74	4.63
Embu	0.14	4.75	4.94	0.16	4.15	4.36	-0.18	9.38	9.44
Garissa	0.02	4.56	4.88	-0.07	5.11	8.074	0.36	4.41	4.56
JKIA	0.28	6.80	6.93	0.31	6.15	6.209	0.41	5.17	5.25
Kakamega	0.72	7.79	8.11	0.54	5.21	6.108	-0.12	1.75	21.1
Kericho	0.33	8.17	8.6	-0.08	9.16	9.376	-0.11	4.05	4.97
Kisii	0.47	5.45	5.76	0.43	3.64	4.006	0.30	3.38	3.82
Kisumu	0.66	5.78	6.07	0.40	3.82	4.214	0.43	3.11	3.46
Kitale	0.76	8.41	8.6	0.18	6.17	7.028	0.01	3.09	3.78
Lamu	0.38	2.09	1.95	0.21	-0.32	1.333	0.49	0.27	0.95
Lodwar	0.04	6.90	6.33	0.22	5.60	6.124	0.08	3.85	5.43
Machakos	0.08	3.06	3.87	0.53	2.61	2.715	0.47	2.84	2.95
Makindu	0.35	5.00	4.89	-0.27	5.02	5.205	0.38	5.51	5.61
Malindi	0.25	0.79	1.55	0.32	2.02	2.196	0.30	0.86	1.36
Mandera	0.01	19.79	25	-0.22	5.18	5.37	0.04	5.16	5.59
Marsabit	-0.24	5.26	5.36	0.44	4.07	4.243	-0.18	5.33	5.54
Meru	-0.08	4.61	4.81	0.10	3.39	3.54	0.49	3.98	4.06
Mombasa	0.11	2.72	2.66	-0.02	2.26	2.604	0.62	2.56	2.68
Moyale	0.10	4.65	4.98	0.14	1.97	3.71	0.02	0.03	1.84

Mtwapa	0.14	0.46	1.28	-0.14	0.24	1.29	0.20	0.06	1.04
Nakuru	0.08	7.61	7.85	0.18	6.24	6.548	-0.23	5.61	6.04
Narok	-0.10	8.10	8.51	0.03	7.14	7.321	0.00	5.00	5.3
Nyeri	-0.27	5.72	6.58	0.49	4.05	4.149	-0.04	3.14	3.35
Thika	-0.22	6.92	7.32	0.05	5.82	5.923	0.27	5.91	6
Voi	0.14	5.30	5.06	-0.12	4.17	4.631	0.53	4.91	5.02
Wajir	-0.04	3.78	3.98	-0.29	3.01	3.425	0.22	3.80	3.93

4.3.2 Measure of the Skill

The results for Frequency Bias Index, Equitable Threat Scores, True Skill Statistics and Hit Rate calculated from 2 by 2 contingency table for the observed and model forecast for the stations used are shown in Tables 6,7 and 8 and Figure 28 and 29.

From Table 6, it is evident that for threshold of 0.5 mm/day and 1 mm/day, the FBI is close to 1 over more station, indicating non biasness, at 0.1 mm/day the model over predict while at threshold of 3mm/day and higher the model under predict the events. This shows that the model may fail to capture extreme event at some location

The ETS results are shown in Table 7 for different stations. Thresholds 0.1, 0.5, and 1 mm/day gave the highest ETS, as compared to the higher thresholds of 3, 5, and 10 mm/day. Therefore, the model has higher skill of forecasting the lower thresholds.

For TSS the same scenario as that of ETS is depicted, where the model performs better at lower thresholds than higher thresholds.

The results from the Hit rate shown in Figure 29 show that in all threshold the percentage correct was above 50% for March-May 2011 seasonal rainfall while, Figure 30, shows that the Hit rate for the month of March was above 50% however, a few stations during April and May had the hit rate less than 50% suggesting that during the two month rainfall at some locations were associated with system that are not captured by the model.

Table 5: Frequency Bias Index (FBI) for Rainfall

Rainfall in mm/day	0.1	0.5	1	3	5	10
Dagoretti	1.83	1.38	1.32	0.47	0.27	0.17
Eldoret	1.43	1.58	1.53	1.91	2.80	3.33
Embu	1.18	1.03	0.88	0.82	0.53	0.17
Garissa	0.75	0.43	0.60	0.00	0.00	0.00
JKIA	2.13	1.43	1.15	0.86	0.50	0.33
Kakamega	1.14	0.92	0.97	0.89	1.10	0.93
Kericho	1.22	1.24	1.23	0.70	0.73	0.71
Kisii	0.94	0.72	0.64	0.43	0.39	0.27
Kisumu	1.17	0.85	0.71	0.54	0.38	0.20
Kitale	1.24	1.19	1.27	0.90	0.68	0.90
Lamu	2.12	2.00	2.11	1.69	1.33	1.00
Lodwar	1.40	1.00	0.75	0.67	2.00	0.00
Machakos	2.79	0.64	0.36	0.43	0.43	0.25
Makindu	2.22	1.75	1.29	0.50	0.00	0.00
Malindi	2.07	2.03	2.19	2.85	2.94	4.20
Mandera	0.75	0.50	0.33	0.50	0.00	0.00
Marsabit	0.94	0.38	0.31	0.29	0.50	0.00
Meru	0.96	0.63	0.36	0.14	0.17	0.14
Mombasa	1.76	1.42	0.96	0.29	0.18	0.33
Moyale	2.24	2.50	3.55	4.43	5.20	7.50
Mtwapa	1.66	1.63	1.87	1.82	1.75	2.33
Nakuru	0.80	0.50	0.48	0.28	0.31	0.33
Narok	1.94	1.00	0.73	0.40	1.00	0.67
Nyeri	1.32	0.91	0.62	0.33	0.17	0.11
Thika	1.63	1.41	1.05	0.45	0.50	0.33
Voi	0.52	0.32	0.31	0.13	0.17	0.00
Wajir	0.78	0.57	0.17	0.00	0.00	0.00

Table 6: Equitable Threat Score for Rainfall

Rainfall in mm/day	0.1	0.5	1	3	5	10
Dagoretti	0.22	0.17	0.22	0.03	0.04	-0.01
Eldoret	0.24	0.23	0.29	0.18	0.14	0.15
Embu	0.15	0.24	0.21	0.14	0.07	0.14
Garissa	0.30	0.03	-0.03	0.00	0.00	0.00
JKIA	0.23	0.14	0.07	0.26	0.18	0.32
Kakamega	0.24	0.28	0.23	0.20	0.20	0.13
Kericho	0.35	0.28	0.23	0.12	0.12	0.22
Kisii	0.25	0.19	0.13	0.09	0.03	0.01
Kisumu	0.11	0.05	0.08	0.20	0.10	-0.02
Kitale	0.24	0.22	0.22	0.14	0.12	-0.01
Lamu	0.13	0.21	0.18	0.20	0.18	0.12
Lodwar	0.30	0.12	0.14	-0.02	-0.01	0.00
Machakos	0.11	0.14	0.03	0.08	0.08	0.24
Makindu	0.07	0.03	0.09	0.18	0.00	0.00
Malindi	0.14	0.12	0.15	0.11	0.12	0.06
Mandera	0.12	-0.03	-0.02	-0.02	0.00	0.00
Marsabit	0.08	0.07	0.09	-0.02	-0.01	0.00
Meru	0.11	0.04	0.07	0.04	0.05	0.13
Mombasa	0.09	0.13	0.17	0.10	-0.02	-0.02
Moyale	0.07	0.04	0.03	0.07	0.05	0.11
Mtwapa	0.09	0.07	0.04	0.09	0.14	-0.01
Nakuru	0.23	0.09	0.11	0.10	0.17	0.32
Narok	0.19	0.20	0.29	0.13	0.22	0.23
Nyeri	0.11	0.16	0.03	0.13	-0.02	-0.01
Thika	0.29	0.25	0.17	0.10	0.16	0.12
Voi	0.04	0.02	0.02	-0.01	-0.01	0.00
Wajir	0.10	0.07	0.06	0.00	0.00	0.00

Table 7: True skill statistics for Rainfall

Rainfall in mm/day	0.1	0.5	1	3	5	10
Dagoretti	0.45	0.32	0.40	0.05	0.06	-0.01
Eldoret	0.43	0.45	0.54	0.42	0.44	0.56
Embu	0.26	0.39	0.34	0.24	0.10	0.17
Garissa	0.05	0.04	-0.04	0.00	0.00	0.00
JKIA	0.53	0.29	0.13	0.38	0.24	0.33
Kakamega	0.39	0.44	0.38	0.32	0.35	0.23
Kericho	0.49	0.43	0.37	0.21	0.20	0.33
Kisii	0.42	0.36	0.25	0.17	0.06	0.02
Kisumu	0.21	0.09	0.14	0.30	0.14	-0.03
Kitale	0.39	0.37	0.39	0.24	0.19	-0.02
Lamu	0.29	0.46	0.41	0.42	0.34	0.21
Lodwar	0.54	0.21	0.22	-0.03	-0.03	0.00
Machakos	0.33	0.21	0.04	0.11	0.11	0.25
Makindu	0.20	0.07	0.18	0.24	0.00	0.00
Malindi	0.29	0.26	0.33	0.33	0.35	0.28
Mandera	0.19	-0.04	-0.03	-0.03	0.00	0.00
Marsabit	0.14	0.11	0.12	-0.03	-0.01	0.00
Meru	0.20	0.07	0.11	0.06	0.07	0.14
Mombasa	0.18	0.25	0.28	0.14	-0.03	-0.03
Moyale	0.19	0.12	0.14	0.33	0.27	0.82
Mtwapa	0.16	0.13	0.09	0.21	0.32	-0.02
Nakuru	0.36	0.15	0.16	0.13	0.21	0.33
Narok	0.43	0.33	0.40	0.17	0.36	0.32
Nyeri	0.19	0.27	0.06	0.17	-0.03	-0.02
Thika	0.52	0.44	0.30	0.13	0.22	0.15
Voi	0.06	0.03	0.03	-0.01	-0.01	0.00
Wajir	0.02	0.10	0.17	0.00	0.00	0.00

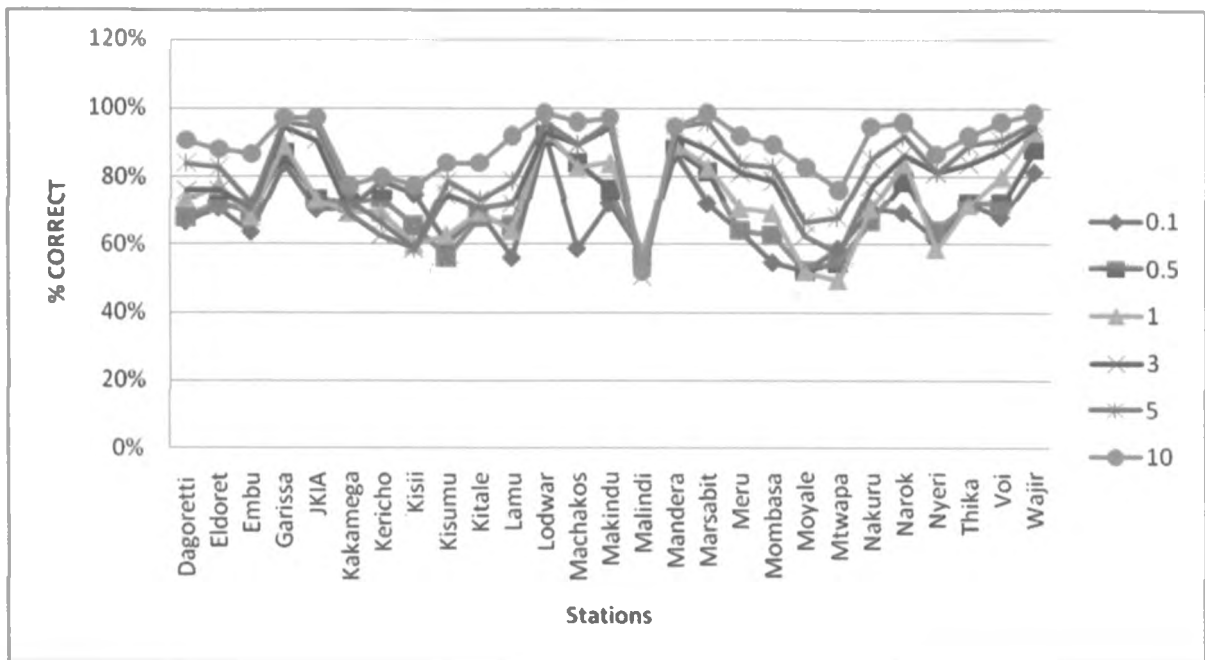


Figure 29: Percentage correct for the forecast for March-May 2011 rainfall season

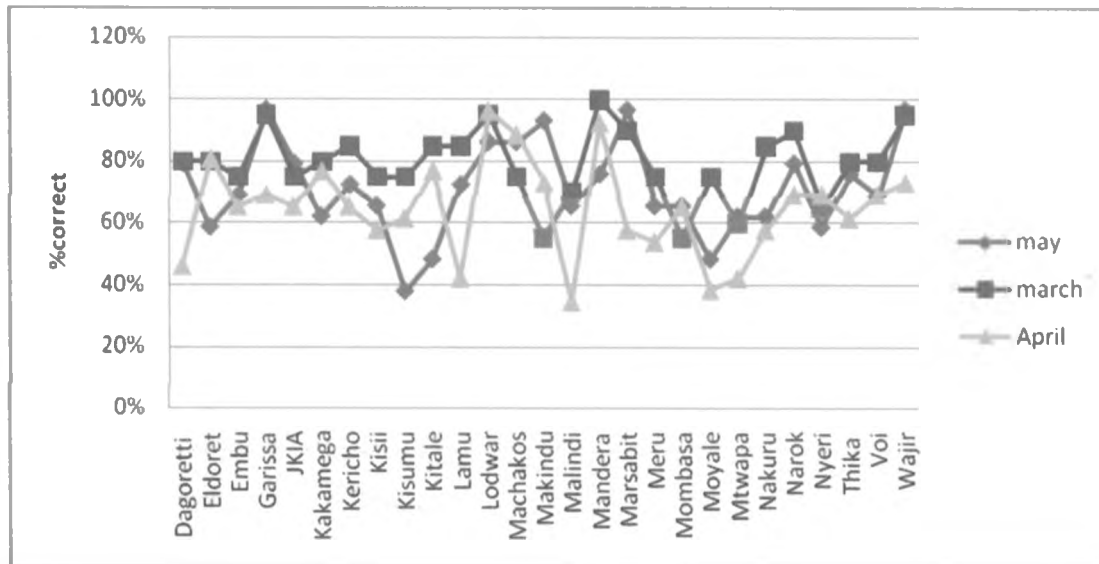


Figure 30: Percentage correct of the forecast rainfall for the month of March-May 2011

CHAPTER FIVE

SUMMARY, CONCLUSIONS AND RECOMMENDATIONS

5.0 Summary

The main objective of the study was to simulate the weather distribution over Kenya using the WRF-EMS model. The verification statistics have been presented for the March-May 2011 seasonal rainfall forecast for WRF-EMS model. The observed rainfall from 27 stations was verified against the model output.

The March to May 2011 seasonal rainfall was highly depressed and poorly distributed, both in time and space, over most parts of the country. This was more so over the North-eastern parts of Kenya and the Coastal strip where most meteorological stations recorded less than 50 percent of their seasonal Long-Term Means (LTMs) for March to May. The rainfall was also characterised by late onset in some parts of the country. A few stations namely Kitale, Embu, Machakos, Kisii, Lodwar, Nakuru, Voi, Kericho and Kakamega, however, recorded rainfall that was within the near-normal category (between 75 and 125% of their seasonal LTMs) but the distribution was also generally poor with a prolonged dry spell in April.

The rainfall and temperature were simulated for the March to May for the year 2011. It was noted that whereas the model reproduced the general spatial distribution pattern of the observed rainfall, during the days when highest rainfall was recorded at some location, the model displaced the location with intense rainfall, such that it under estimated at some locations and over estimated at others. The model simulates the spatial distribution of temperature fairly well, though there were over estimation over a few locations. The deficiency in computation of rainfall, also affect the temperature, since temperature is dependent among other things on latent heat release.

The correlation between the observed and forecasted rainfall for the entire season was generally higher over most locations. On monthly basis, the correlation was higher during March as compared to April and May. The correlation between the observed and forecasted temperature

showed a similar pattern as rainfall although the values were much lower. The Absolute Mean Error and Root Mean squer Error for both Rainfall and Temperature were low over most locations, the errors in the forecasteing of rainfall and temperature values were generally low.

The results from the analysis of FBI, ETS, and TSS showed that the model has the highest skill for threshold of less than 1mm/day, and the skill decreased with increase in the threshold. The hit rate for the entire season was above 50% over most stations. On monthly basis, the hit rate was highest in March and decreased during April and May with a few stations going below 50%. During April and May there was low spatial coherence in rainfall due to sub-synoptic activities which were not well captured by the model.

5.1. Conclusion

From the spatial distribution of rainfall it can be seen that whereas WRF-EMS Model reproduced the general pattern, during days where heavy rainfall occurs, it tends to displace the location of the observed heavy rainfall as shown in figures 19 and 20. The model simulates the spatial distribution of temperature fairly well even though it overestimated in most cases..

Overall the model has skills in forecasting both rainfall and temperature. However the skill of forecasting the accuracy of specified rainfall threshold decrease with increasing threshold. Therefore, while the accuracy of the model-generated rainfall and temperature increases with decreasing threshold. WRF-EMS may be used with confidence for predictions of rainfall in most of the study area. It may however fail to predict the occurrence of storm, especially over the coastal and western area.

5.2 Recommendations

Although the model performed very well in the simulation of the spatial and temporal pattern of rainfall and temperature for most stations, it failed to replicate exact amount and location of intense rainfall. There is therefore need to improve its performance over the domain through reviewing the parameterization of small scale physical processes.

In this study, the skill of the model to simulate the weather pattern over a short range was done. There is need to examine its ability to simulate weather on the medium and long range scale.

One of the most important components of numerical weather prediction is initialization. Initialization is dependent on the quality of the observed data. The network of stations over the Kenya region is very sparse. For this reason, policy makers should work towards increasing the number of stations. Observations of weather parameters need to be put on grids for easier comparison with the model outputs.

DEPT OF METEOROLOGY UNIVERSITY
OF NAIROBI

6.0 ACKNOWLEDGEMENTS

I wish to acknowledge, first of all, the Almighty God for giving me the opportunity, strength and ability to carry out this research.

I also take this opportunity to thank my supervisors (Dr. Ininda and Dr. Opijah) for the advice, direction and support they extended to me during the study. The same also goes to the entire staff of the Department of Meteorology at the University.

I also wish to thank The University of Nairobi for funding my MSc studies.

I also wish to register my appreciation to Mr Vincent Sakwa, Mr. Mungai both of Kenya Meteorological Department, for their guidance during the course of the research.

Finally, to my family, and friends for the encouragement and support they accorded me during the entire period of the course.

7.0 REFERENCES

- Mishra, A. K. and Krishnamurti, T. N., 2008: Current status of multimodal super ensemble and operational NWP forecast of the Indian summer monsoon. *J. Earth System Science*, **116**, 5, 369-384.
- Anderson, J. L., 1996: A method for producing and evaluating probabilistic forecasts from ensemble model integrations. *J. climate*, **9**, 1518-1530.
- Anna, G. and Francis. L., 2001: Verification of precipitation forecasts over the Alpine region using a high density observing network. *J. Weather and Forecasting*, **17** 239 – 249.
- Anyamba E. K., 1992: Some properties of a 20–30 day oscillation in tropical convection. *African. Met. Soc.* **1**, 1-19.
- Atger, F. 2001: Verification of intense precipitation forecasts from single models and ensemble prediction systems, *Processes Geophys.*, **8**, 401-417
- Bock O. and Nuret M, 2009: Verification of NWP model analyses and radiosonde humidity data with GPS precipitable water vapor estimates during AMMA. *Weather and Forecasting*, DOI:10.1175/2009WAF2222239.1.
- Brian A. C., Westrick, K. J. and Mass, C. F. 1998: Evaluation of MM5 and ETA – 10 Precipitation forecasts over the pacific North West during the cool season. *Weather and Forecasting*, **14**,137 -153.
- Briggs, W. M. and Levine, R. A., 1997: Wavelets and field forecast verification. *Monthly Weather Review*, **125**, 1329–1341.
- Brooks, H. E., and Kay, M. 1998: Objective limits on forecasting skill of rare events. *Preprints, 19th Conf. On Severe Local Storms*, Minneapolis, Amer. Meteor. Soc., 552-555
- Chessa P A., and Lalaurette, F., 2001: Verification of the ECMWF Ensemble Prediction System Forecasts: A Study of Large-Scale Patterns. *Weather and Forecasting*, **16**, 611-619

Clark, M. P., and Lauren E. H., 2004: Use of Medium-Range Numerical Weather Prediction Model Output to Produce Forecasts of Stream flow. *J. Hydrometeorology*, **5**, 15-32

Das, S. A., Mitra, K., Iyengar, G. R. and Singh, J. 2002: Skill of Medium-Range Forecasts over the Indian Monsoon Region Using Different Parameterizations of Deep Convection. *Weather and Forecasting*, **17**, 1194-1210

Deb S. K., Srivastava T. P. and Kishtawal, C. M. , 2008: The WRF model performance for the simulation of heavy precipitating events over Ahmedabad during August 2006. *J. Earth System Science*, **117**, 589-602

Ebert, E. E. And McBride, J.L., 1999: Verification of Quantitative Precipitation Forecasts from Operational Numerical Weather Prediction Models over Australia. *Weather and Forecasting*, **15**, 103-121.

Ebert, E. E., and McBride, J. L., 2000: Verification of precipitation in weather systems: determination of systematic errors. *J. Hydrometeorolog.*, **239**, 179-202.

Epstein, E. S., 1969: Stochastic-dynamic prediction. *Tellus*, **21**, 739-759.

Ferrier, B. S., Lin, Y., Black, T., Rogers, E. and DiMego, G., Implementation of a new grid-scale cloud and precipitation scheme in the NCEP Eta model. In 15th Conference on Numerical Weather Prediction, San Antonio, TX, Preprints, American Meteorological Society, 2002, pp. 280-283.

Findlater, J., 1971: Mean monthly airflow at low levels over the western Indian oceans. Geophys Memo. No. **115**, HMSO London, UK

Folland, C. K., Owen, J. M. N. And Colman, A. 1991: Prediction of seasonal rainfall in the Sahel region using empirical and dynamical methods, *Weather and Forecasting*, **10**, 21-56

Ghelli, A., and Lalaurette, F., 2000: Verifying precipitation forecasts using upscaled observations. *ECMWF Newsletter*, **87**, 9-17.

Gitutu, J. M., 2006: A Comparative Verification of Precipitation Forecasts for Selected Numerical Weather Prediction Models over Kenya. *Msc. Thesis*, Dept. of Meteorology University of Nairobi.

Grell, G. A. and Devenyi, D., A generalized approach to parameterizing convection combining ensemble and data assimilation techniques. *Geophys. Res. Lett.*, 2002, **29**, 1693.

Harvey S., 2008: The accuracy of weather forecasts for Melbourne, Australia. *Meteorology. Appl.* **15**, 65–71

Hoffman, R. N., Liu. Z., Louis, J. F. and Grassotti, C. 1995: Distortion representation of forecast errors. *Mon. Wea. Rev.*, **123**, 2758-2770.

Indeje, M., 1993: A numerical study of the effects of the roughness length on the mesoscale flow patterns over Kenya; *MSc. Thesis*, University of Nairobi.

Indenje M, F., Semazzi, H.M. and Ogallo, L. .J. 2000: Enso Signals in East African Rainfall Seasons. *Int.j. Climatol.*, **1** 19-46.

Janjic ZI. 1996: The Surface Layer in the NCEP Eta Model. *11th Conference on NWP*. American Meteorological Society: Norfolk, VA; 354–355

Janjic, Z.I. 2002: Nonsingular Implementation of the Mellor-Yamada Level 2.5 Scheme in the NCEP Meso model. NCEP Office Note, No. 437, 61.

Janjic, Z.I. 2003: A nonhydrostatic model based on a new approach. *Meteorology and Atmospheric Physics* **82**: 271–285

Krishnamurti, R., and Krishnamurti, T. N. 1979: Surface meteorology during one hundred days of GATE, *J. Deep-Sea Res.*, Supplement II, **26**, 29–62.

Krishnamurti, T. N., Mishra, A. K., Chakraborty, A., and Rajeevan, M. 2009: Improving Global Model Precipitation Forecasts over India Using Downscaling and the FSU Superensemble. Part I: 1–5-Day Forecasts. *Monthly Weather Review*, **137**, 2713-2735

- Lacis, A. A. and Hansen, J.E. 197:. A parameterization for the absorption of solar radiation in the earth's atmosphere. *J. Atmospheric Science* **31**: 118–133
- Litta, J., Mohantya, U. and Bhanb, S.. 2010: Numerical Simulation of a tornado over Ludhiana (India) using WRF-NM model. *Meteorological Applications* **17**: 64–75 (2010)
- Mahoney, J.L., Brown, B.G., Hart, J E. and C. Fischer, 2002: Using verification techniques to evaluate differences among convective forecasts. Preprint 16th Conference on Probability and Statistics in the Atmospheric Sciences, 14-18 January, Orlando, FL, *J. American Meteorological Society, Boston*, 12-19.
- Min, S. J., Legutke S., Hense, A, Cubasch, U, Kwon, W and Schlese, U., 2006: East Asian Climate Change in the 21st Century as Simulated by the Coupled Climate Model ECHO-G under IPCC SRES Scenarios. *J. Meteorological Society of Japan* **84**,1
- Mukabana, J. R. and Pielke, R. A. 1996: Investigating the influence of synoptic scale monsoonal winds and meso – scale circulations on diurnal weather patterns over Kenya using a meso – scale numerical model. *Mon. Wea. Rev.* **124**, 222 – 243.
- Mukabana, J.R., 1992: Numerical simulation of the influence of large-scale Monsoon flow on weather patterns over Kenya using a three –dimensional limited area model. *Ph.D Dissertation, Dept of met., University of Nairobi, Kenya.*
- Murphy A. H. And Winkler, R.L. 1987: A general framework for forecast verification. *Weather Review*, **115**, 1330-1338.
- Murphy A. H., 1991: Forecast verification: Its complexity and dimensionality. *Monthly Weather Review*, **119**, 1590-1601.
- Murphy, A. H., 1993: What is a good forecast? An essay on the nature of goodness in weather forecasting. *Monthly Weather Review*, **8**, 281-293

Murphy, A.H., 1988: Skill scores based on the mean square error and their relationships to the correlation coefficient. *Mon. Wea. Rev.* **116**, 2417-2424.

Murphy, A.H., and Winkler, L. 1987: A general framework for forecast verification. *Mon. wea. Rev.*, **115**, 1330-1338

Mutemi J. N., Ogallo, L., Krishnamurti, T. N., Mishra, A. K. and Vijaya Kumar, T. S. V. 2006: Multimodel based super ensemble forecasts for short and medium range NWP over various regions of Africa. *Meteorol Atmos Phys*, **95**, 87-113

Nigel, R., 2008: Assessing the spatial and temporal variation in the skill of precipitation forecasts from an NWP model. *Meteorol. Appl.* **15**, 163-169

Ogallo, L. J., 1988: Relationship between Seasonal Rainfall in East Africa and Southern Oscillation. *J. Climatol.*, **8**, 34-43.

Ogallo, L. J., 1989: The spatial and temporal patterns of the East African seasonal rainfall derived from principal component analysis. *Int. J. Climatol.* **9**, 145-165.

Ogallo, L. J., Janowiak J.E, and Halpert, M.S. 1988: Teleconnections between seasonal rainfall over East Africa and global sea surface temperature Anomalies. *J.meteor.soc.Japan*, **66**, 807-821.

Renwick, J. A. and Craig, S., 2001: Southern Hemisphere Medium-Range Forecast Skill and Predictability: A Comparison of Two Operational Models. *Mon. Wea. Rev.*, **129**, 2377-2391

Richard. O. A and Semazzi, F. H. M. 2003: Climate variability over the Greater Horn of Africa based on NCAR AGCM ensemble. *J. Theoretical and Applied Climatology*, **86**, 34-62

Roulin, E. and Stéphane, V., 2005: Skill of Medium-Range Hydrological Ensemble Predictions. *J. Hydrometeor*, **6**, 729-744

Sakwa V.N., 2006: Assessment of the Skill of the High Resolution Regional Model in the Simulation of Airflow and Rainfall over East Africa. *Msc. Thesis*, Dept. of Meteorology UoN

Schwarzkop, M.D. and Fels, S.B., 1991. The simplified exchange method revisited: an accurate, rapid method for computations of infrared cooling rates and fluxes. *J. Geophysical Research* **96**: 9075–9096.

Someshwar, D., Raghavendra. A., Gopal R. I., Saji M., Gupta, M. D., John, P.G., Rajagopal, E. N. and Surya K. D., 2008: Skills of different mesoscale models over Indian region during monsoon season: Forecast errors. *J. Earth System Science*, **117**, 5, 603-620

Taylor, P.K., 2001: Intercomparison and validation of ocean-atmosphere energy flux fields. Joint WCRP/SCOR Working Group on Air-Sea Fluxes Final Rep., WCRP-112, WMO/TD-No. **1036**, 306.

Vyzilova, N., 2001: Rainfall anomalies over East Africa and interannual variation of large-scale moisture transport over Indian Ocean. Atlas conferences, PP-PEP III

WMO, 2002: Standardised verification System, SVS: for long-range forecasts, LRF: *Manual on the GDPS*, WMO-No. 485: 1.

Yonas, B. G., 2009: Evaluation of Three Numerical Weather Prediction Models for Short and Medium Range Agrohydrological Applications *J. Water Resources Management*, **24**, 1005-1028.